

# Oestrogen promotes KCNQ1 potassium channel endocytosis and postendocytic trafficking in colonic epithelium

Raphael Rapetti-Mauss<sup>1</sup>, Fiona O'Mahony<sup>1</sup>, Francisco V. Sepulveda<sup>2</sup>, Valerie Urbach<sup>1</sup> and Brian J. Harvey<sup>1</sup>

<sup>1</sup>Department of Molecular Medicine, Education and Research Centre, Royal College of Surgeons in Ireland, Beaumont Hospital PO Box 9063, Dublin 9, Republic of Ireland

<sup>2</sup>Centro de Estudios Científicos CECs, 512 Arturo Prat, Valdivia, Chile

## Key points

- Oestrogen (E<sub>2</sub>) exposure leads to a decrease in both Cl<sup>-</sup> secretion and KCNQ1 current. This inhibition is maintained by a rapid and sustained retrieval of the channel from the plasma membrane.
- The E<sub>2</sub>-stimulated internalization of KCNQ1 occurs via a dynamin- and clathrin-dependent mechanism.
- KCNQ1 is recycled back to the cell membrane via Rab4 and Rab11 rather than being degraded.
- The signalling pathway activated by E<sub>2</sub> and leading to KCNQ1 internalization involves a signalling cascade, in which the activation of protein kinase Cδ induces the phosphorylation of AMP-dependent kinase. Oestrogen stimulated an increase in the association of KCNQ1 with the ubiquitin ligase Nedd4.2.
- The findings provide evidence for a hormone-stimulated regulation of KCNQ1 surface density in colonic epithelium. Moreover, this study complements the understanding of the mechanisms for E<sub>2</sub>-induced inhibition of KCNQ1 previously described, and provides new insights on hormonal regulation of ion channel retrieval from the plasma membrane.

**Abstract** The cAMP-regulated potassium channel KCNQ1:KCNE3 plays an essential role in trans-epithelial Cl<sup>-</sup> secretion. Recycling of K<sup>+</sup> across the basolateral membrane provides the driving force necessary to maintain apical Cl<sup>-</sup> secretion. The steroid hormone oestrogen (17β-oestradiol; E<sub>2</sub>), produces a female-specific antisecretory response in rat distal colon through the inhibition of the KCNQ1:KCNE3 channel. It has previously been shown that rapid inhibition of the channel conductance results from E<sub>2</sub>-induced uncoupling of the KCNE3 regulatory subunit from the KCNQ1 channel pore complex. The purpose of this study was to determine the mechanism required for sustained inhibition of the channel function. We found that E<sub>2</sub> plays a role in regulation of KCNQ1 cell membrane abundance by endocytosis. Using chamber experiments have shown that E<sub>2</sub> inhibits both Cl<sup>-</sup> secretion and KCNQ1 current in a colonic cell line, HT29cl.19A, when cultured as a confluent epithelium. Following E<sub>2</sub> treatment, KCNQ1 was retrieved from the plasma membrane by a clathrin-mediated endocytosis, which involved the association between KCNQ1 and the clathrin adaptor, AP-2. Following endocytosis, KCNQ1 was accumulated in early endosomes. Following E<sub>2</sub>-induced endocytosis, rather than being degraded, KCNQ1 was recycled by a biphasic mechanism involving Rab4 and Rab11. Protein kinase Cδ and AMP-dependent kinase were rapidly phosphorylated in response to E<sub>2</sub> on their activating phosphorylation sites, Ser643 and Thr172, respectively (as previously shown). Both kinases are

necessary for the  $E_2$ -induced endocytosis, because  $E_2$  failed to induce KCNQ1 internalization following pretreatment with specific inhibitors of both protein kinase C $\delta$  and AMP-dependent kinase. The ubiquitin ligase Nedd4.2 binds KCNQ1 in response to  $E_2$  to induce channel internalization. This study has provided the first demonstration of hormonal regulation of KCNQ1 trafficking. In conclusion, we propose that internalization of KCNQ1 is a key event in the sustained antisecretory response to oestrogen.

(Received 15 January 2013; accepted after revision 19 March 2013; first published online 25 March 2013)

**Corresponding author** B. J. Harvey: Department of Molecular Medicine, RCSI-ERC, Beaumont Hospital, PO Box 9063, Dublin 9, Ireland. Email: bjpharvey@rcsi.ie

**Abbreviations** AMPK, AMP-dependent kinase; AP-2  $\mu 2$ , adaptor protein 2 subunit  $\mu 2$ ; CHX, cycloheximide; Comp-C, compound-C; CPZ, chlorpromazine; Ctl, control; Dyna, dynasore;  $E_2$ , oestrogen 17 $\beta$ -oestradiol; EEA-1, early endosome antigen-1; ER, oestrogen receptor; FSK, forskolin; GSH, glutathione; HERG, ether-a-go-go-related gene; IB, immunoblot; IP, immunoprecipitation;  $I_{sc}$ , short-circuit current;  $I_K$ , basolateral potassium current; LPA-1, lysophosphatidic acid receptor 1; Nedd4.2, neural precursor cell-expressed developmentally downregulated protein 4.2; Nyst, nystatin; O.C., overlap coefficient; PKA, protein kinase A; PKC $\delta$ , protein kinase C $\delta$ ; Rot, rottlerin; TER, transepithelial resistance.

## Introduction

In the distal colon, chloride and fluid secretion are essential to maintain a hydrated mucosa and contribute to the regulation of whole-body fluid and electrolyte homeostasis. Chloride transport from the serosa to the mucosa creates an osmotic gradient favouring water movement into the lumen. Chloride secretion is a complex mechanism involving several ion channels and transporters and is tightly regulated by hormones and signalling peptides in order to avoid dehydration of the colonic mucosa or diarrhea. Chloride is transported into the cell basolaterally through the  $Na^+K^+2Cl^-$  cotransporter (NKCC1), and is secreted across the apical membrane through the cystic fibrosis transmembrane regulator. Secretion of  $Cl^-$  is driven by the activity of  $Na^+K^+ATPase$  that actively pumps  $Na^+$  from the cell. The electrochemical driving force for  $Cl^-$  secretion is provided by  $K^+$  recycling across the basolateral membrane via  $K^+$  channels. Furthermore, these channels are responsible for hyperpolarization of the membrane electrical potential difference required to maintain  $Cl^-$  secretion (Barrett & Keely, 2000).

The rapid antisecretory action of the biologically active oestrogen, 17 $\beta$ -oestradiol ( $E_2$ ), has previously been described in female rat distal colonic crypts (Condliffe *et al.* 2001). The classical response to  $E_2$  involves binding of the hormone to its specific intracellular receptor, ER $\alpha$  or ER $\beta$ , and its subsequent translocation to the nucleus, where it regulates gene expression. However, it is now well accepted that in addition to this genomic response,  $E_2$  exerts a rapid, non-genomic effect via plasma membrane receptors (Levin, 2009; Prossnitz & Barton, 2011). It has been demonstrated that  $E_2$  inhibits basal and secretagogue-induced  $Cl^-$  secretion in a rapid and gender-specific manner via the modulation of the basolateral  $K^+$  channel

KCNQ1:KCNE3. 17 $\beta$ -oestradiol-mediated inhibition of KCNQ1 channel activity occurs indirectly via activation of protein kinase C $\delta$  (PKC $\delta$ ) and protein kinase A (PKA);  $E_2$  activates both kinases, which in turn phosphorylates the KCNQ1:KCNE3 channel complex, resulting in dissociation of the regulatory subunit KCNE3 and a collapse in the channel conductance (O'Mahony *et al.* 2007).

The voltage-gated, cAMP-regulated potassium channel KCNQ1 is an important component of basolateral  $K^+$  recycling in colonic epithelium (Preston *et al.* 2010). KCNQ1 can associate with each of the five members of the  $\beta$ -regulatory subunit KCNE family. The electrophysiological and pharmacological properties of the channel change drastically depending on the KCNE subunit involved (Melman *et al.* 2002; Bendahhou *et al.* 2005). This property allows KCNQ1 to be involved in a wide range of different functions when differentially expressed with one of the KCNE subunits in a tissue-specific manner (Jespersen *et al.* 2005). In the heart, the KCNQ1:KCNE1 complex, also known as IKs, is essential in the repolarization phase of the cardiac action potential (Splawski *et al.* 1997). When expressed with KCNE2, KCNQ1 controls acid secretion in gastric epithelium (Heitzmann & Warth, 2007). KCNE4 seems to downregulate KCNQ1 activity in overexpression systems (Manderfield *et al.* 2009). In the distal colon, where KCNQ1 is expressed with KCNE3, this association turns KCNQ1 into a constitutively activated  $K^+$  channel (Schroeder *et al.* 2000). In different tissues, KCNQ1 has been shown to be regulated by an intracellular increase in cAMP. It has been well described how KCNQ1 current is regulated by PKA-induced phosphorylation, especially in the heart when expressed with KCNE1 (Marx *et al.* 2002). These two mechanisms of regulation of KCNQ1 are well documented. Recently, however, a growing number of

studies have reported the importance of channel surface density regulation in physiology and disease (Guo *et al.* 2009). The mechanism governing the channel surface density as well as the physiological outcome of this phenomenon remains poorly understood for KCNQ1, especially in colonic epithelium. The surface density of ion channels is the result of the balance between forward trafficking (exocytosis) and retrograde trafficking (endocytosis). Rab GTPases have been shown to play a major role in the regulation of endocytosis of several potassium channels, including Kv1.5 (Zadeh *et al.* 2008), ether-a-go-go-related gene (HERG; Guo *et al.* 2009) and KCNQ1 (Seeböhm *et al.* 2007). Indeed, KCNQ1 has been shown to undergo Rab5-mediated endocytosis. Moreover, Seeböhm *et al.* (2007) demonstrated that following endocytosis the serum- and glucocorticoid-inducible kinase 1 enhanced KCNQ1 recycling via Rab11.

Recently, we outlined the molecular mechanism explaining the action of  $E_2$  on KCNQ1 involving an  $E_2$ -dependent dissociation of KCNQ1 from KCNE3 leading to a decrease in KCNQ1 activity (Alzamora *et al.* 2011a). Considering that regulation of membrane density appears to be a key regulator of ion channel activity, in the present study we hypothesized that  $E_2$  plays a role in KCNQ1 surface density regulation so as to maintain a sustained inhibition in  $Cl^-$  secretion following its initial rapid inhibition. Here, our results demonstrate a rapid onset and sustained effect of  $E_2$  on KCNQ1 surface expression correlated with a decrease in KCNQ1 current as well as a decrease in  $Cl^-$  secretion. The  $E_2$ -induced internalization of KCNQ1 appeared to be dependent on a clathrin-mediated endocytosis. Moreover, following  $E_2$  exposure KCNQ1 was found to colocalize with Rab5 and EEA-1 positive vesicles. Interestingly, internalized KCNQ1 is recycled rather than degraded, through a mechanism involving Rab4 and Rab11. The  $E_2$ -stimulated endocytosis of KCNQ1 was dependent on PKC $\delta$ , activation of AMP-dependent kinase (AMPK) and an increase in KCNQ1–Nedd4.2 association, suggesting a subsequent ubiquitination of KCNQ1 and channel internalization.

## Methods

### Ethical approval

Experiments carried out on female Sprague–Dawley rats were performed on post-mortem isolated tissue from excised distal colon. The project was approved by the Royal College of Surgeons in Ireland local ethics committee in compliance with legal regulations existing in the Republic of Ireland Animal Welfare Acts.

### Materials

Rabbit anti-phospho-PKC $\delta$  (Ser643) and rabbit anti-phospho-AMPK (Thr172; 1:1000 dilution), were

obtained from Cell Signaling Technology (Hitchin, UK). Mouse anti-adaptor protein 2 subunit  $\mu 2$  (anti-AP-2  $\mu 2$ ; Immunofluorescence 1:100, Western blotting 1:250), mouse anti-Rab5, mouse anti-Rab4, mouse anti-Rab11 and mouse anti-EEA-1 (1:100 dilution), were obtained from BD Transduction Laboratories (Dorchester, UK). Rabbit anti-KCNQ1 (WB 1:2000) was from Sigma-Aldrich (Dublin, Ireland), rabbit anti-KCNQ1 (IF 1:100) was obtained from Abcam (Cambridge, UK), as was mouse anti-Nedd4.2 antibody. Rabbit anti-KCNE3 (1:100 dilution) was obtained from Alamone Labs (Jerusalem, Israel). Secondary antibodies were as follows: Alexa Fluor<sup>®</sup> 488 nm-conjugated goat anti-rabbit (1:4000 dilution) and Alexa Fluor<sup>®</sup> 568-conjugated goat anti-mouse (1:2000 dilution) from Invitrogen (Carlsbad, CA, USA); and anti-rabbit and anti-mouse HRP-linked secondary antibodies were obtained from Cell Signaling Technology (Beverly, MA, USA). All drugs and chemicals were obtained from Sigma-Aldrich unless specified as follows: HMR-1556 was kindly provided by Dr Uwe Gerlach (Aventis Pharma Deutschland, Frankfurt-am-Main, Germany); dynasore, dorsomorphin dihydrochloride (compound-C) and bisindolylmaleimide-I (BIS-I) were obtained from Tocris Bioscience (Bristol, UK); and rottlerin, chlorpromazine (CPZ) and cycloheximide were obtained from Calbiochem (Nottingham, UK).

### Cell culture

The HT29cl.19A cell line was a kind gift from Dr Christian Laboisse (EA4273 University of Nantes, Nantes, France) (Augeron & Laboisse, 1984). HT29 cells are a well-described model for colonic secretion studies. The HT29cl.19A clone is representative of non-aggressive adenocarcinoma. The cells were cultured in Dulbecco's modified Eagle's medium supplemented with 10% fetal bovine serum, penicillin–streptomycin and 1 mM glutamine. Cells were grown on insert were semi-permeable supports from Millipore (Cork, Ireland) until the transepithelial resistance (TER) reached  $\sim 1 \text{ k}\Omega \text{ cm}^{-2}$ . The culture media were changed every 2–3 days. For 24 h prior to each experiment, the cells were starved in 0% serum media without Phenol Red.

### Animals

All experiments using animals were conducted in accordance with the Department of Environment legislation and were approved by the Ethics committee of the Royal College of Surgeons in Ireland. Sprague–Dawley rats (300–350 g) were kept on a 12 h light–12 h dark cycle and were given *ad libitum* access to food and water. Halothane was delivered by Inhalation using an induction chamber, cervical smears were carried after the anesthesia

and before the rats were killed to minimize wastage of animals. Cervical smears were obtained from female rats, and the stage of the oestrous cycle was determined. Three-month-old female rats were used at estrus (maximal impact of  $E_2$  *in vivo*). The distal colon was removed, and faecal contents were rinsed off. Colonic crypts were isolated using the technique described in the next subsection.

### Isolation of colonic crypts

The rat distal colon was removed, everted on a glass rod, and placed in crypt isolation buffer, pH 7.4 (96 mM NaCl, 1.5 mM KCl, 10 mM HEPES-Tris, 27 mM EDTA, 55 mM sorbitol, 44 mM sucrose and 1 mM dithiothreitol) at room temperature for 40 min. The crypts were detached after the incubation by vigorous shaking, followed by centrifugation at 1000g for 10 min. The pellet of crypts obtained was resuspended in Krebs solution (140 mM NaCl, 5 mM KCl, 1 mM  $MgCl_2$ , 2 mM  $CaCl_2$ , 10 mM HEPES, 10 mM Tris-HCl and 10 mM glucose). The purity of isolated intact crypts was verified under bright-field microscopy and was typically 90–100% without crypt fracture.

### Electrophysiological measurements

HT29cl.19A cell monolayers grown on permeable supports (Millipore, surface = 0.6 cm<sup>2</sup>) were mounted in Ussing chambers (Physiologic Instruments, San Diego, CA, USA) in order to measure the transepithelial  $Cl^-$  secretion. The transepithelial potential difference was clamped to 0 mV and monitored for changes in transepithelial short-circuit current ( $\Delta I_{sc}$ ) using an EVC4000 voltage-clamp apparatus (World Precision Instruments, Aston, UK). The  $I_{sc}$  was recorded using Ag–AgCl electrodes in 3 M KCl agar bridges. Apical and basolateral chambers were filled with Ringer's solution containing (mM): 120 NaCl, 1.2  $CaCl_2$ , 1.2  $MgCl_2$ , 25  $NaHCO_3$ , 2.4  $K_2HPO_4$ , 0.4  $KH_2PO_4$  and 10 glucose. In these conditions, secretagogue-induced  $\Delta I_{sc}$  across HT29cl.19A monolayers is wholly reflective of changes in electrogenic  $Cl^-$  secretion. Results were normalized to an area of 1 cm<sup>2</sup> and were expressed as  $\Delta I_{sc}$  (in microamperes per square centimetre).

Basolateral membrane  $K^+$  conductance was measured by permeabilizing the apical membrane of HT29cl.19A cell monolayers with 50  $\mu M$  of amphotericin B (Kirk & Dawson, 1983). An apical-to-basolateral  $K^+$  gradient was imposed by filling the apical chamber with a solution containing (mM): 140 potassium gluconate, 1.25  $CaCl_2$ , 0.4  $MgCl_2$ , 3.3  $KH_2PO_4$ , 0.5  $K_2HPO_4$ , 25  $HCO_3^-$  and 10 glucose and the basolateral chamber with a solution containing (mM): 137 sodium gluconate, 5 potassium gluconate, 1.25  $CaCl_2$ , 0.4  $MgCl_2$ , 3.3  $KH_2PO_4$ , 0.5  $K_2HPO_4$ ,  $NaHCO_3$  and 10 glucose. Ouabain (100  $\mu M$ ) was added basolaterally to inhibit  $Na^+ - K^+ - ATPase$  pump

activity. In these conditions, changes in  $I_{sc}$  are wholly reflective of changes in basolateral  $K^+$  conductance ( $I_K$ ).

### Cell lysates

After the particular treatment for each experiment, for example, oestrogen treatment or PKC inhibitor treatment. HT29cl.19A cells were washed three times in ice-cold PBS; then a Radio Immuno Precipitation Assay (RIPA) lysis buffer [50 mM Tris-HCl, 150 mM NaCl, 1% Nonidet-P40 (NP-40), 0.1% SDS, 0.5% sodium deoxycholate, phosphatase inhibitor cocktail (1:100) and protease inhibitor tablet (Roche, Clairecastle, Ireland; one tablet for 10 ml)] or Immuno-precipitation (IP) lysis buffer [50 mM Tris-HCl, 150 mM NaCl, 1% NP-40, 3% glycerol, 2 mM EDTA, 2 mM EGTA, phosphatase inhibitor cocktail (1:100) and protease inhibitor tablet (Roche; one tablet for 10 ml)] were applied to the cells for 30 min at 4°C. The samples were scraped and left at 4°C for another 30 min in lysis buffer. Thereafter, the samples were sonicated (3 × 10 s), centrifuged at 15,000 g for 15 min, and the supernatant was collected. Protein concentration was measured using the Bradford protein assay (Bio-Rad laboratories, Hemel Hempstead, UK) according to the manufacturer's instructions.

### Western blotting

Samples were subjected to 8% SDS-PAGE, after which the proteins were transferred onto a nitrocellulose membrane. Membranes were incubated in blocking buffer (5% low-fat milk in TBS-T or 5% bovine serum albumin in Tris-buffered saline-Tween 20 (TBS-T), depending on the primary antibody) for 1 h at room temperature. Thereafter, the membrane was incubated with the primary antibody diluted in the blocking buffer overnight at 4°C. The membrane was then washed three times for 15 min in TBS-T prior to incubation with the HRP-conjugated secondary antibody in blocking buffer for 1 h at room temperature. After washing three times for 15 min in TBS-T, the membrane was incubated with ECL plus (GE Healthcare, Cambridge, UK) prior to detection.

### Cell surface protein biotinylation

Serum-starved cells were treated with 10 nM  $E_2$  for 15 min at 37°C. The treated cells were then washed twice with ice-cold PBS and incubated with 1 mg ml<sup>-1</sup> sulfo-NHS-SS-biotin (Pierce) in PBS for 30 min at 4°C under agitation (120 r.p.m.). Unreacted biotin was quenched and removed with quenching buffer (200 mM glycine). Cells were then washed in PBS and lysed with IP lysis buffer. Extracts were clarified by centrifugation (15,000 g for 15 min at 4°C), and then biotinylated proteins were isolated from the total cell extract by pull-down with streptavidin-conjugated sepharose beads

(Pierce, Rockford, IL, USA). Samples were incubated with beads overnight at 4°C, and then the beads were washed six times with IP lysis buffer. Proteins were eluted from the sepharose beads by cleavage of the S–S bound by SDS sample buffer. Thereafter, the proteins were subjected to Western blotting.

### Biotin internalization and recycling assay

After serum starvation for 24 h, cell surface proteins were biotinylated using 1 mg ml<sup>-1</sup> membrane-impermeable sulfo-NHS-SS-biotin (Pierce) in PBS with calcium and magnesium (Sigma) supplemented with 10 mM glucose (PBS+) at 4°C for 30 min under agitation at 120 r.p.m. Free biotin was then quenched with 200 mM glycine in PBS+ for 15 min, followed by washing with ice-cold PBS+ once. Cells were all incubated at 37°C for 60 min to allow internalization and treated with E<sub>2</sub> for the indicated times. After stimulation, residual surface biotin was stripped off with glutathione (GSH) buffer (50 mM glutathione, 75 mM NaCl, 1 mM EDTA, 1% bovine serum albumin and 0.75% 10 N NaOH) three times for 10 min. Thereafter, the glutathione was quenched by iodocetamide buffer (5 mg ml<sup>-1</sup>) for 15 min to terminate the reaction and washed three times in PBS+ prior to being lysed. Streptavidin was added to the samples to precipitate internalized biotin-labelled proteins. Eluates from beads were subjected to Western blot. For the recycling assay, after biotinylation, cells were incubated with 10 nM E<sub>2</sub> for 15 min to drive internalization of biotinylated proteins at 37°C. The cells were then cooled on ice, and the remaining biotinylated proteins at the cell surface were stripped off with glutathione buffer. Internalized biotinylated receptors were protected from biotin stripping. Then the cells were incubated at 37°C for different times to allow recycling of internalized labelled proteins. A second round of stripping with glutathione buffer was done to remove biotin from the cell surface. Unrecycled labelled proteins were detected by streptavidin pull-down followed by KCNQ1 immunoblotting.

### Immunoprecipitation

Following E<sub>2</sub> treatment and protein extraction in IP lysis buffer, samples were precleared with AminoLink beads plus coupling resin (co-immunoprecipitation kit; Pierce) in order to reduce non-specific binding. Anti-KCNQ1 antibody was immobilized on Aminolink plus coupling resin beads using sodium cyanobromide as a cross-linking reagent (75 mM). Precleared samples were added to the KCNQ1–beads complex and incubated overnight at 4°C on a rotator. The beads were then washed with IP lysis buffer four times, and then eluted with elution buffer pH 2.8 (Pierce). Samples were subjected to SDS-PAGE and Western blotting assay. In order to

control the specificity of the co-immunoprecipitation, negative controls were carried out following the co-immunoprecipitation protocol described above. The KCNQ1 antibodies coupled with beads without proteins were subjected to the co-immunoprecipitation protocol to control the presence of antibody in the final eluate (Ab alone). The KCNQ1 antibody was then omitted, and the beads were incubated with the proteins to control for non-specific binding to the beads (beads). Finally, 5 µl of normal rabbit serum was incubated with the beads instead of KCNQ1 antibody as an IgG control (IgG).

### Immunofluorescence

Cells grown on a permeable support (Millipore, Cork, Ireland) were treated as specified in the Results. Thereafter, the cells were fixed in 4% paraformaldehyde in PBS for 10 min at room temperature. Cells were then permeabilized in 0.4% Triton in PBS, then blocked for 2 h in blocking buffer (10% bovine serum albumin and 10% normal goat serum). The cells were incubated in primary antibodies diluted in blocking buffer for 1 h at room temperature (anti-KCNQ1 or anti-KCNE3), or overnight at 4°C (AP-2 µ2, Rab5, Rab4, Rab11, or EEA-1). Secondary antibodies were diluted in blocking buffer and applied for 45 min at room temperature. For co-immunostaining, antibodies were added sequentially, and an additional blocking step was performed after the first secondary antibody incubation. After incubation with antibodies, three 5 min washes were performed in washing buffer (0.1% Triton in PBS). Cells were finally mounted in Vectashield (Vector Laboratories, Burlingame, CA, USA) containing 4',6'-diamidino-2-phenylindole (DAPI) stain.

### Confocal microscopy and imaging

Laser scanning confocal microscopy was performed using the Zeiss LSM 710 confocal system. Images were acquired using a ×63 or ×40 oil-immersion objectives (Zeiss), with a pinhole size of 0.8 µm and a pixel format of 1024 × 1024. Line averaging was used to reduce noise.

### Data analysis and statistics

Densitometric analyses of the data from Western blots were performed using Adobe Photoshop CS3. The area around each specific band was selected by drawing a line around the band. The mean intensity value was then multiplied by the pixel value. For colocalization analysis, the overlap coefficient (Manders *et al.* 1993) was calculated using Zen 2008 software. The results are given as the mean ± SEM for a series of an indicated number of experiments. The statistical significance was established using one-way ANOVA followed by Tukey's *post hoc* test or Student's paired *t* test where relevant. GraphPad Prism5

(GraphPad Software, San Diego, CA, USA) was used for statistical analyses.

## Results

### Oestrogen reduces forskolin-stimulated KCNQ1 current in HT29cl.19A cells

Previous studies from our laboratory established that  $17\beta$ -oestradiol ( $E_2$ ) reduces the forskolin-evoked  $Cl^-$  secretion in female rat colonic crypts (Condliffe *et al.* 2001; O'Mahony *et al.* 2007). In the present study, we first examined whether the  $E_2$  antisecretory effect was reproducible in HT29cl.19A monolayers. Confluent HT29cl.19A monolayers were mounted in Ussing chambers, and then subjected to an  $E_2$  or KCNQ1 inhibitor (chromanol 293B) treatment (Fig. 1A and B). After 15 min treatment, the cells were stimulated by the addition of  $10 \mu M$  forskolin. Chromanol 293B ( $10 \mu M$ ; a specific KCNQ1 inhibitor) reduced the forskolin-stimulated  $I_{sc}$  by  $65 \pm 4\%$  ( $n = 6$ ,  $P < 0.001$ ). It is now well described that KCNQ1:KCNE3 potassium channel activity is crucial for cAMP-stimulated  $Cl^-$  secretion in colonic epithelium (Preston *et al.* 2010).  $17\beta$ -oestradiol reduced the effect of forskolin on  $I_{sc}$  by  $30 \pm 6\%$  ( $n = 6$ ,  $P < 0.05$ ) in the HT29cl.19A cells.

KCNQ1 has been identified as an  $E_2$  target in the rapid inhibition of  $Cl^-$  secretion in female rat colon (O'Mahony *et al.* 2007). In order to confirm the  $E_2$  inhibitory effect on KCNQ1 activity in HT29cl.19A monolayers, the apical membrane was perforated using  $50 \mu M$  amphotericin B (Fig. 1C and D). An apical-to-basolateral  $K^+$  gradient was applied to the epithelium, and the  $I_{sc}$  was recorded. In these conditions, the  $I_{sc}$  is mainly driven by the basolateral  $K^+$  current ( $I_{sc} = I_K$ ). As expected, the KCNQ1 channel inhibitors chromanol 293B and HMR-1556 strongly inhibited the forskolin-induced current by  $87.5 \pm 1.6$  and  $86.3 \pm 5.4\%$ , respectively ( $n = 5$ ,  $P < 0.001$ ). This result demonstrates that the  $\Delta I_K$  observed after forskolin treatment is mostly due to KCNQ1:KCNE3 activation. We also noted a weak but significant inhibition of the basal  $I_K$  by  $15 \pm 3.5\%$  ( $n = 5$ ,  $P < 0.05$ ) after chromanol treatment. Treatment with  $E_2$  (15 min) reduced the forskolin-induced KCNQ1 current by  $45.8 \pm 8.2\%$  ( $n = 5$ ,  $P < 0.05$ ). There was no effect on basal  $I_K$  upon  $E_2$  treatment.

In a previous study, we reported that the mechanism of KCNQ1 inhibition by  $E_2$  involved a rapid dissociation between the channel and the KCNE3 subunit (Alzamora *et al.* 2011a). In order to assay whether the effect of  $E_2$  on  $I_K$  is only transient or whether it can be sustained over a longer period, we pretreated the HT29cl.19A cells with  $E_2$  ( $10 \text{ nM}$ ) for 2 h at  $37^\circ C$  in the incubator prior to mounting the monolayer in Ussing chambers. The basolateral  $I_K$  was recorded as described in the Methods in the continuous presence of  $E_2$  ( $10 \text{ nM}$ ) on the basolateral side

of the chamber. After 2 h of oestrogen treatment, the effect on  $I_K$  observed after 15 min acute treatment was sustained ( $40.7 \pm 3.4\%$ ). This result suggests that KCNQ1 inhibition after  $E_2$  treatment is maintained over at least 2 h. Interestingly, we observed a significant inhibitory effect of  $E_2$  on basal basolateral  $I_K$  after 2 h of  $E_2$  treatment ( $16 \pm 3\%$  compared with the control,  $n = 5$ ,  $P < 0.05$ ; Fig. 1E and F).

### Oestrogen promotes KCNQ1 internalization in colonic epithelium

In order to investigate whether the effect of  $E_2$  on KCNQ1 current is due to a decrease in KCNQ1 protein abundance at the plasma membrane, the effect of  $E_2$  on KCNQ1 trafficking was examined in female rat colonic crypts and in HT29cl.19A confluent monolayers. As reported previously, the antisecretory response to oestrogen is sex specific and estrous-cycle dependent (Condliffe *et al.* 2001; O'Mahony *et al.* 2007; Alzamora *et al.* 2011a). No effects of oestrogen on  $Cl^-$  secretion or KCNQ1 trafficking were observed in colonic crypts isolated from male rats, and the studies here were therefore confined to female rats in oestrus. As expected, KCNQ1 is mostly expressed at the basolateral membrane in rat colonic crypts (Fig. 2A). After crypt isolation, rat crypts were subjected to  $E_2$  treatment. KCNQ1 immunostaining showed that 30 min of  $E_2$  treatment induced retrieval of KCNQ1 from the membrane (Fig. 2B). Confocal images of KCNQ1 staining revealed that in untreated cells, KCNQ1 undergoes a minimal constitutive internalization, observed as intracellular accumulation of the fluorescent dye that could correspond to endocytic vesicles. After  $E_2$  treatment, a stimulated internalization was noted after 15 min and sustained until at least 60 min. The KCNQ1 staining in control conditions was clearly localized mainly at the plasma membrane. During  $E_2$  treatment, KCNQ1 staining appeared as punctate pools below the plasma membrane, indicating movement from the membrane to the cytosol (Fig. 2C).

This observation was further confirmed by quantitative analysis of KCNQ1 internalization using a biotin internalization assay. Surface proteins were biotinylated and allowed to internalize during  $E_2$  treatment for different times. Internalized biotin-labelled KCNQ1 was detected by Western blotting. The biotin assay confirmed that KCNQ1 undergoes a constitutive internalization, because a weak amount of internalized KCNQ1 can be detected in the untreated conditions.  $17\beta$ -oestradiol treatment stimulated KCNQ1 internalization (Fig. 2D and E); after 15 min treatment, the quantity of internalized KCNQ1 was more than doubled ( $226 \pm 11.5\%$ ) compared with the control, as well as after 30 ( $264 \pm 19\%$ ) and 60 min ( $248 \pm 12\%$ ,  $n = 5$ ,  $P < 0.001$ ). The biotin internalization assay demonstrates that the increase in cytosolic KCNQ1

is not due to a defective insertion but is a result of rapid retrieval of the channel from the plasma membrane.

**Oestrogen-induced internalization of KCNQ1 occurs via clathrin-coated vesicles**

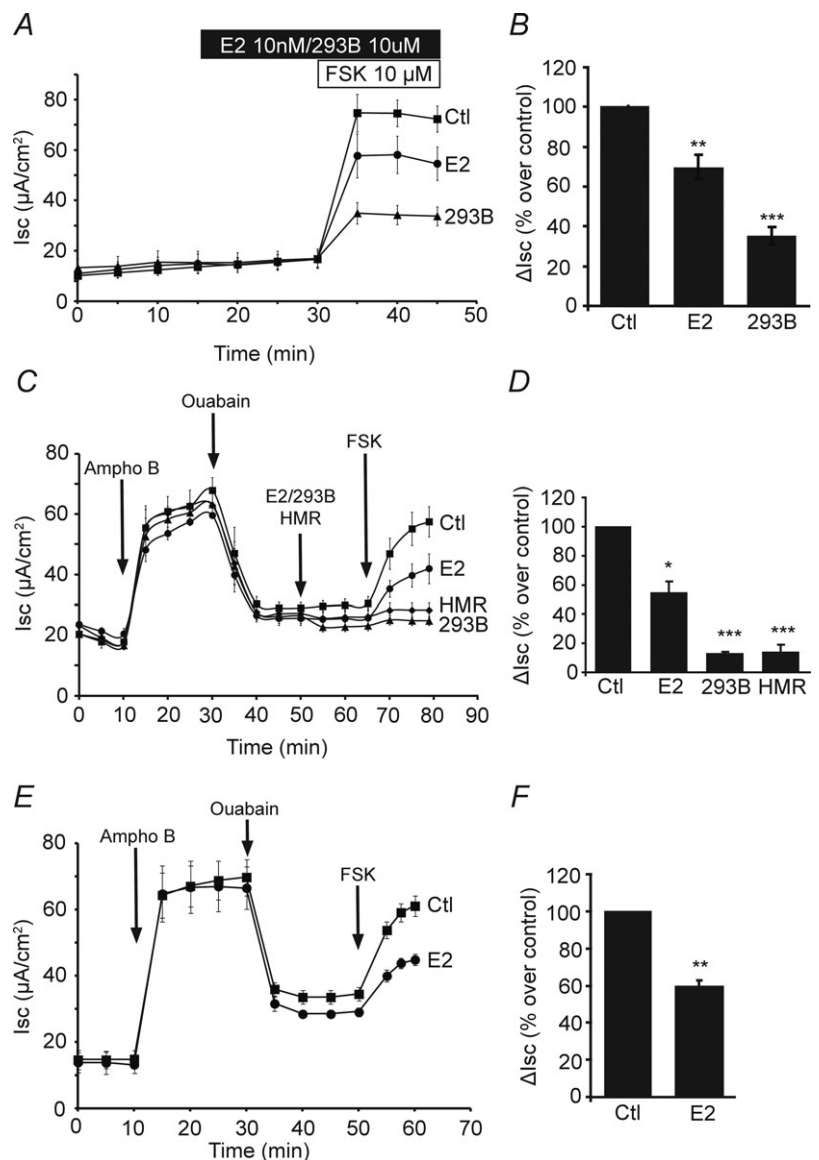
To date, few studies have investigated KCNQ1 internalization in heterologous systems (Seeböhm *et al.* 2007; Andersen *et al.* 2011; 2012; Kanda *et al.* 2011). However, so far there are no data reporting the mechanisms for spontaneous or regulated KCNQ1 internalization in any tissue. Here, we determined the molecular mechanisms for E<sub>2</sub>-induced internalization of KCNQ1 in colonic epithelium. In order to investigate possible kinase and small G protein mechanisms for KCNQ1 internalization, we first treated the HT29cl.19A mono-

layers with different internalization pathway inhibitors. There are three main mechanisms underlying surface proteins internalization, namely clathrin-mediated endocytosis, caveolin-mediated endocytosis and clathrin- and caveolin-independent endocytosis. The GTPase dynamin is essential to endocytosis, because this protein allows the vesicle to be separated from the plasma membrane. We studied the effect of pharmacological inhibition of these three trafficking mechanisms on the E<sub>2</sub>-induced KCNQ1 internalization.

Cells were pretreated with 30 μM chlorpromazine (CPZ) for 30 min, 15 μM nystatin for 30 min or 80 μM dynasore for 10 min and then treated with E<sub>2</sub> in the continuous presence of inhibitors. We observed that both dynasore and CPZ were able to reverse the effect of E<sub>2</sub>, while nystatin failed to counteract

**Figure 1. Effect of 17β-oestradiol (E<sub>2</sub>) on forskolin-stimulated KCNQ1 current in HT29cl.19A cells**

**A**, recording from Ussing chamber experiments showing short-circuit currents (*I*<sub>sc</sub>) across control HT29cl.19A monolayers (■) and monolayers treated with 10 nM E<sub>2</sub> (●) or 10 μM chromanol 293B (▲). Cells were treated basolaterally with E<sub>2</sub> or chromanol 293B for 15 min, after which forskolin (FSK; 10 μM) was added, as indicated by the horizontal bars. **B**, mean change in forskolin-induced *I*<sub>sc</sub> in E<sub>2</sub>-treated (E<sub>2</sub>) or chromanol-treated (293B) conditions expressed as a percentage of the control (Ctl) value. Values were measured at the FSK plateau, 30 min after E<sub>2</sub> or 293B exposure. Values are shown as means + SEM; \*\**P* < 0.01, \*\*\**P* < 0.001 (*n* = 6). **C**, *I*<sub>sc</sub> recording from HT29cl.19A monolayers in the presence of an apical-to-basolateral K<sup>+</sup> gradient. Epithelia were mounted in Ussing chambers, after which 50 μM amphotericin B (Ampho B) was added apically to reveal the ionic currents flowing across the basolateral membrane. The contribution of the Na<sup>+</sup>-K<sup>+</sup>-ATPase pump current to the basolateral membrane current was revealed using ouabain (10 μM). Cells were then treated with E<sub>2</sub> (10 nM; ●) or with the KCNQ1 inhibitors chromanol 293B (10 μM; ▲) or HMR-1556 (HMR; 10 μM; ◆) for 15 min or left untreated (control; ■). Finally, KCNQ1 current was stimulated by addition of forskolin (10 μM). **D**, mean change in forskolin-stimulated *I*<sub>sc</sub> in the different conditions (control and E<sub>2</sub>, chromanol or HMR treated) expressed as a percentage of the control value. Values were measured at the FSK plateau, 30 min after E<sub>2</sub> or 293B/HMR exposure. Values are shown as means + SEM; \**P* < 0.05, \*\*\**P* < 0.001 (*n* = 5). **E**, epithelia were pretreated for 2 h with 10 nM E<sub>2</sub> (●) or untreated (■) in Ussing chambers. The basolateral K<sup>+</sup> currents were recorded as previously described. **F**, mean change in forskolin-stimulated *I*<sub>sc</sub>. Values were measured at the FSK plateau, 3 h after E<sub>2</sub> exposure and are shown as means + SEM; \*\**P* < 0.01 (*n* = 5).



the effect of  $E_2$  on KCNQ1 endocytosis (Fig. 3A and B).

In order to confirm the role of clathrin-mediated endocytosis in KCNQ1 internalization,  $E_2$ -treated cells were subjected to a costaining for KCNQ1 and AP-2  $\mu 2$  (adaptor protein 2 subunit  $\mu 2$ ), which is a major component of the clathrin-mediated endocytosis machinery, because this particular subunit can associate with protein containing a Yxx $\Phi$  motif (where  $\Phi$  is a hydrophobic residue). KCNQ1 contains several possible motifs and especially the well-known YxxL endocytic motif in its intracellular domain. This experiment revealed that after 10 min of  $E_2$  treatment a clear colocalization of KCNQ1 and AP2  $\mu 2$  was observed on the edge of the cells (Fig. 3C). The pixel overlap coefficient between KCNQ1 and AP2  $\mu 2$  staining was  $0.28 \pm 0.04$  in control conditions,  $0.77 \pm 0.01$  ( $P < 0.001$ ) after 10 min  $E_2$ , and  $0.6 \pm 0.01$  ( $n = 4$ ,  $P < 0.01$ ) after 15 min  $E_2$  (Fig. 3D). Interestingly, after 15 min  $E_2$  exposure

there was less costaining on the edge of the cell, and vesicular staining could be distinguished in the cytosol. The co-immunoprecipitation study of KCNQ1 with AP2  $\mu 2$  revealed a clear increase ( $195.3 \pm 18\%$ ,  $n = 4$ ,  $P < 0.01$ ) in KCNQ1–AP2  $\mu 2$  association after  $E_2$  treatment (Fig. 3E). These results are consistent with the confocal colocalization assay.

### KCNQ1 endocytosis is mediated by Rab5 and leads to an accumulation of KCNQ1 in early endosomes

Protein internalization is a complex mechanism involving different chaperone proteins, which sort the cargo proteins into different endocytic routes. Very little is known about KCNQ1 endocytosis in colonic tissue. It has been demonstrated that in cardiac tissue KCNQ1 endocytosis is dependent on the small GTPase, Rab5 (Sebohm *et al.* 2007). Rab5 is essential in early steps of protein

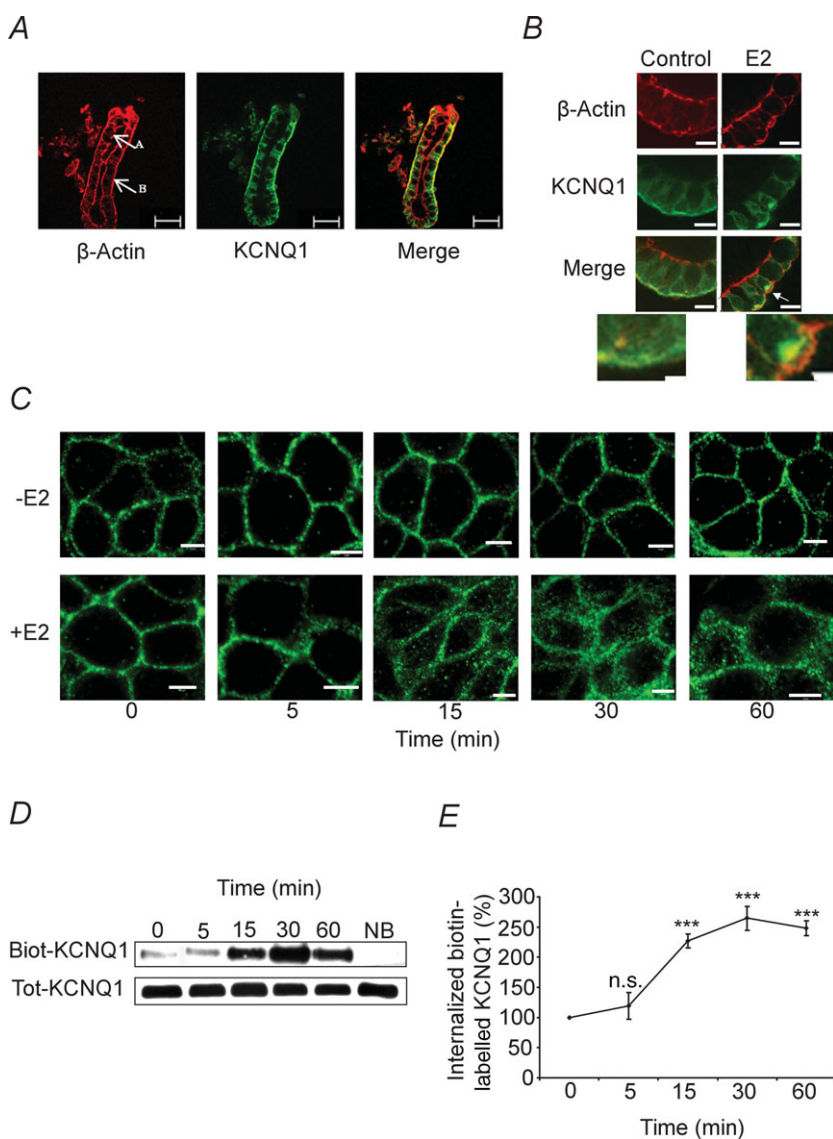


**Figure 2. 17 $\beta$ -oestradiol induces internalization of KCNQ1 in HT29cl.19A cells and female rat distal colonic crypts**  
 A, confocal images of isolated rat colonic crypts. Red shows the  $\beta$ -actin staining and green indicates KCNQ1 staining. 'A' indicates the apical membrane and 'B' the basolateral membrane. Scale bars represent 10  $\mu$ m.  
 B, confocal images showing the effect of  $E_2$  treatment (10 nM) for 30 min on KCNQ1 subcellular localization in rat colonic crypts. Images are representative of three different experiments. Scale bars represent 2  $\mu$ m.  
 C, time course of KCNQ1 internalization revealed by confocal microscopy in HT29cl.19A cells. Top panels show the untreated control. Bottom panels show the effects of treatment with  $E_2$  (10 nM) for the indicated times. Images are representative of five independent experiments (four different fields of view per experiment). Scale bars represent 5  $\mu$ m.  
 D and E show the results of the biotin–KCNQ1 internalization assay. Data are presented as an increase in cytosolic biotin-labelled KCNQ1 accumulation, corresponding to a decrease in membrane-bound biotin–KCNQ1. Biotinylated cell surface proteins were allowed to internalize for the  $E_2$  treatment times indicated. Internalized biotin-labelled KCNQ1 was assayed by Western blot.  $n = 5$ ; \*\*\* $P < 0.001$  versus control by one-way ANOVA followed by Tukey's *post hoc* test. Abbreviations: NB, no biotin added; and n.s., non-significant.



internalization, particularly to permit the sequestration of cargo protein in clathrin-coated pits and fusion of vesicles with early endosomes (Somsel Rodman & Wandinger-Ness, 2000). In order to investigate further how KCNQ1 is internalized after E<sub>2</sub> treatment in colonic tissue, we studied the subcellular localization of KCNQ1.

Co-immunostaining studies revealed that E<sub>2</sub> stimulated the colocalization of KCNQ1 with Rab5 (Fig. 4A and B). 17β-oestradiol treatment (15 min) rapidly increased the number of colocalized pixels by twofold [overlap coefficient (O.C.): control, 0.3 ± 0.03 and E<sub>2</sub>, 0.67 ± 0.02, n = 4, P < 0.001], which was sustained after 30 min (O.C. = 0.73 ± 0.01). This result strongly suggests a role for Rab5 in KCNQ1 endocytosis. Subsequently, the Rab5-mediated endocytosis KCNQ1 was accumulated in early endosomes. The increase in pixel colocalization between KCNQ1 staining and the early endosome

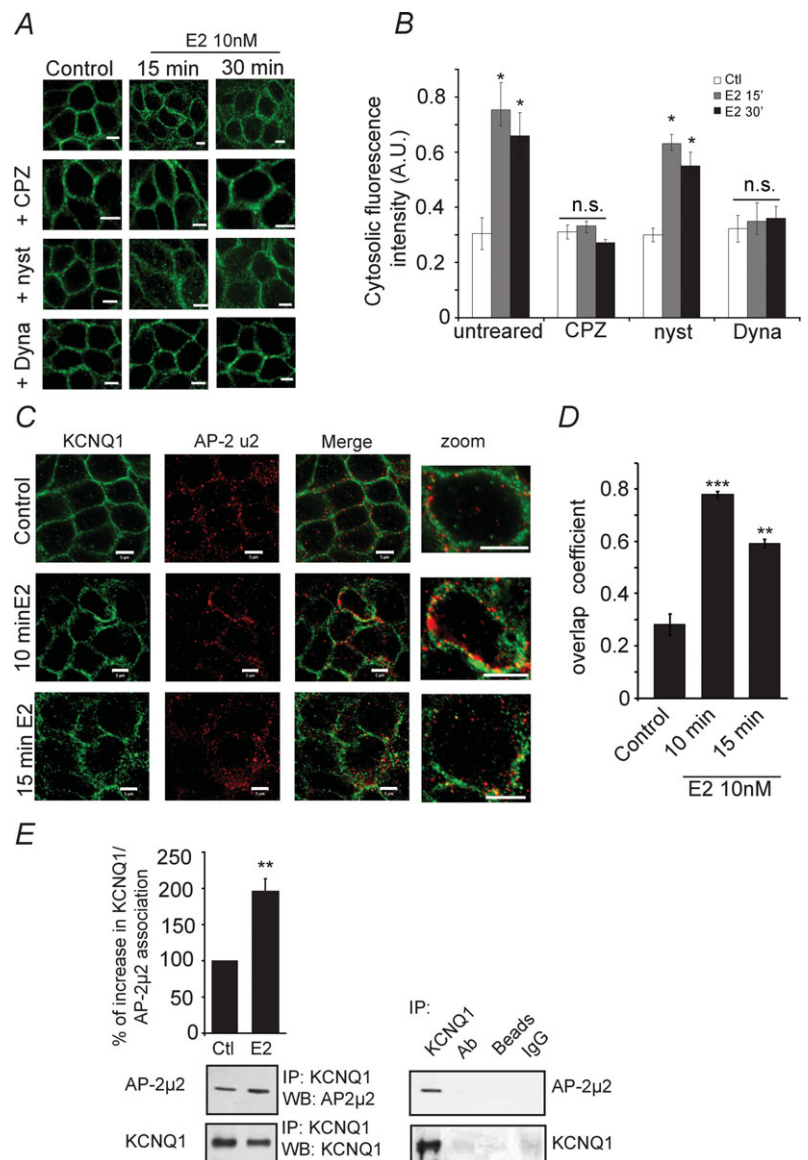
antigen-1 (EEA-1) staining after E<sub>2</sub> exposure (O.C.: control, 0.30 ± 0.07 and E<sub>2</sub>, 0.60 ± 0.04, n = 4, P < 0.01), suggested that E<sub>2</sub> stimulated an accumulation of KCNQ1 in early endosomes (Fig. 4C and D). We confirmed this result in female rat colonic crypts, where KCNQ1 was also accumulated in early endosomes following E<sub>2</sub> exposure (O.C.: control, 0.21 ± 0.01 and E<sub>2</sub>, 0.61 ± 0.02 n = 3, P < 0.01; Fig. 4E and F).

### KCNQ1 is recycled rather than degraded after oestrogen-induced internalization

In order to determine the fate of endocytosed KCNQ1, we first examined the total expression level of KCNQ1 upon prolonged E<sub>2</sub> treatment. Cells were treated with cycloheximide to prevent any protein neosynthesis. Immunoblot analysis was carried out using a specific KCNQ1

**Figure 3. Mechanism of 17β-oestradiol-induced KCNQ1 internalization in HT29cl.19A cells**

**A**, confocal images of an HT29cl.19A monolayer stained with a KCNQ1-specific antibody. Cells were pretreated with the following: chlorpromazine, a clathrin-dependent endocytosis inhibitor (CPZ; 30 μM, 30 min); nystatin, a caveolin-dependent endocytosis inhibitor (Nyst; 15 μM, 30 min); or dynasore, a dynamin inhibitor (Dyna; 80 μM, 10 min) and then treated with 10 nM E<sub>2</sub> for 15 or 30 min in the continuous presence of inhibitors. Scale bars represent 5 μm (n = 3). **B**, quantification of intracellular fluorescence intensity image staining in **A** using Zeiss Zen 2008 software. **C**, colocalization of adaptor protein 2 subunit μ2 (AP-2 μ2; red) and KCNQ1 (green) after 10 or 15 min E<sub>2</sub> treatment (n = 4). Scale bars represent 5 μm. **D**, quantification of AP-2 μ2 and KCNQ1 colocalization using the pixel overlap coefficient. Values are shown as means ± SEM; \*\*P < 0.01, \*\*\*P < 0.001, n = 4. Images were analysed with Zeiss Zen 2008 software. **E**, cells were treated with 10 nM E<sub>2</sub> for 10 min and then protein samples were subjected to immunoprecipitation using a specific KCNQ1 antibody. Then a Western blot was performed to detect AP-2 μ2. KCNQ1 was used as a loading control to normalize AP-2 μ2 for quantification. Different controls were performed to ensure the quality of the co-immunoprecipitation, namely KCNQ1 antibody was added to the beads without proteins (Ab), beads were incubated with proteins but without antibody (Beads), and rabbit IgG was added to the beads instead of KCNQ1 antibody then incubated with proteins (IgG). Values are shown as normalized means ± SEM, \*\*P < 0.01, n = 4. Abbreviations: IB, immunoblot; and IP, immunoprecipitation.



antibody. Over 6 h of  $E_2$  treatment, the amount of KCNQ1 expression remained unchanged (Fig. 5A).

Based on this result, we hypothesized that KCNQ1 was recycled back to the membrane after  $E_2$  treatment. To address this hypothesis, we employed the biotin recycling assay in Methods section. This experiment revealed several novel outcomes. A subset of internalized KCNQ1 was rapidly recycled to the membrane 15 min after internalization ( $30 \pm 4.4\%$  of internalized KCNQ1,  $n = 6$ ,  $P < 0.05$ ). Following 2 h after internalization, there was no significant difference in channel recycling compared with the 15 min duration ( $40 \pm 14\%$  of internalized KCNQ1). This result suggests that the amount of KCNQ1 recycled is constant over a 2 h period. Following 4 h after internalization, we observed a significant recycling of KCNQ1 ( $70 \pm 5\%$ ,  $n = 6$ ,  $P < 0.001$ ). Taken together, these experiments suggest that KCNQ1 is recycled back to

the membrane after 4 h and that the recycling event occurs by two different pathways. One is rapid and occurs in 15 min and the other slow, occurring after 4 h. Moreover, these results indicate that KCNQ1 is sequestered in intracellular compartments for at least 2 h after internalization (Fig. 5B).

Two major Rab GTPases regulate protein recycling; Rab4 controls fast recycling, and Rab11 (Somsel Rodman & Wandinger-Ness, 2000) controls the slow recycling pathway through the recycling endosomes. KCNQ1 colocalized with Rab4 at least 15 min after  $E_2$  treatment (Fig. 5C and D). Rab11 showed no significant increase in colocalization with KCNQ1 after 30 min but did show colocalization 120 min after  $E_2$  treatment. Interestingly, after 4 h of  $E_2$  treatment KCNQ1 and Rab11 were no longer colocalized, and KCNQ1 seemed to be recycled back to the plasma membrane (Fig. 5E and F). When cells

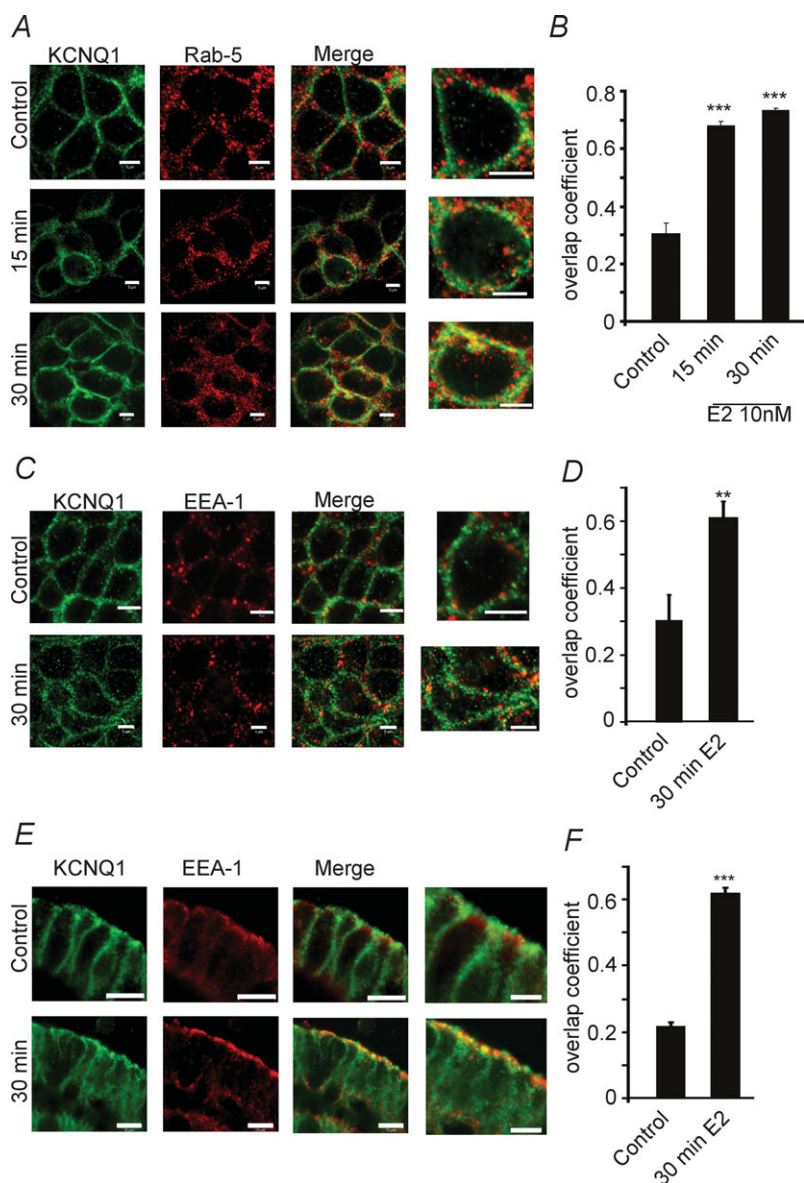


**Figure 4. Localization of KCNQ1 following  $17\beta$ -oestradiol-induced internalization in HT29cl.19A cells and female rat colonic crypts**

A, confocal images showing colocalization of KCNQ1 (green) and Rab5 (red) in control conditions or after 15 and 30 min  $E_2$  treatment. Colocalization of KCNQ1 and Rab5 appears in yellow. Scale bars represent  $5 \mu\text{m}$  ( $n = 4$ ). B, quantification of KCNQ1 colocalization with Rab5 using the pixel overlap coefficient. Values are shown as means  $\pm$  SEM; \*\*\* $P < 0.001$ ;  $n = 4$ . C, confocal images showing colocalization of KCNQ1 staining (green) with early endosome antigen-1 (EEA-1) staining (red) following vehicle treatment as a control and after 30 min  $E_2$  treatment. Scale bars represent  $5 \mu\text{m}$ . D, quantification of KCNQ1 colocalization with EEA-1; \*\* $P < 0.01$ ,  $n = 4$ . E, confocal images showing KCNQ1 colocalization with EEA-1 in female rat colonic crypts after vehicle and 30 min  $E_2$  treatment. Scale bars represent  $10 \mu\text{m}$ . F, quantification of KCNQ1 colocalization with EEA-1 in female rat colonic crypts; \*\* $P < 0.01$ ,  $n = 3$ .

were vehicle treated, the colocalization between KCNQ1 and Rab11 did not change over the experimental period (Supporting information, Fig. S1A and B).

**Oestrogen-induced internalization of KCNQ1 is dependent on PKCδ and AMPK activation**

We previously demonstrated in female rat colonic crypts that PKCδ was the main kinase involved in the E<sub>2</sub>-induced inhibition of KCNQ1 (O'Mahony *et al.* 2007). In order to determine whether PKCδ also plays a role in KCNQ1 internalization, we tested the effect of E<sub>2</sub> treatment on PKCδ phosphorylation in HT29cl.19A cells. Following 2 min of E<sub>2</sub> treatment, PKCδ phosphorylation increased by 287 ± 51% (*n* = 4, *P* < 0.05). As shown in Fig. 6A, this effect was sustained for 15 min, after which time the

phosphorylation of PKCδ returned to the control value within 30 min of E<sub>2</sub> exposure (as previously shown).

Recent studies have shown a correlation between KCNQ1 internalization and the activation of AMPK (Alzamora *et al.* 2010; Alesutan *et al.* 2011a; Andersen *et al.* 2012). We hypothesized that this kinase could have a role in oestrogen-induced KCNQ1 internalization. In order to address this hypothesis, we carried out a Western blotting analysis of the effect of E<sub>2</sub> treatment on AMPK phosphorylation (Fig. 6B). Following 2 min of E<sub>2</sub> treatment, AMPK phosphorylation rapidly increased by 232 ± 24% (*n* = 5, *P* < 0.05).

In order to demonstrate the involvement of these two kinases in KCNQ1 internalization, we used immunostaining and confocal images (Fig. 6C). A KCNQ1-specific antibody was used to stain E<sub>2</sub>-treated

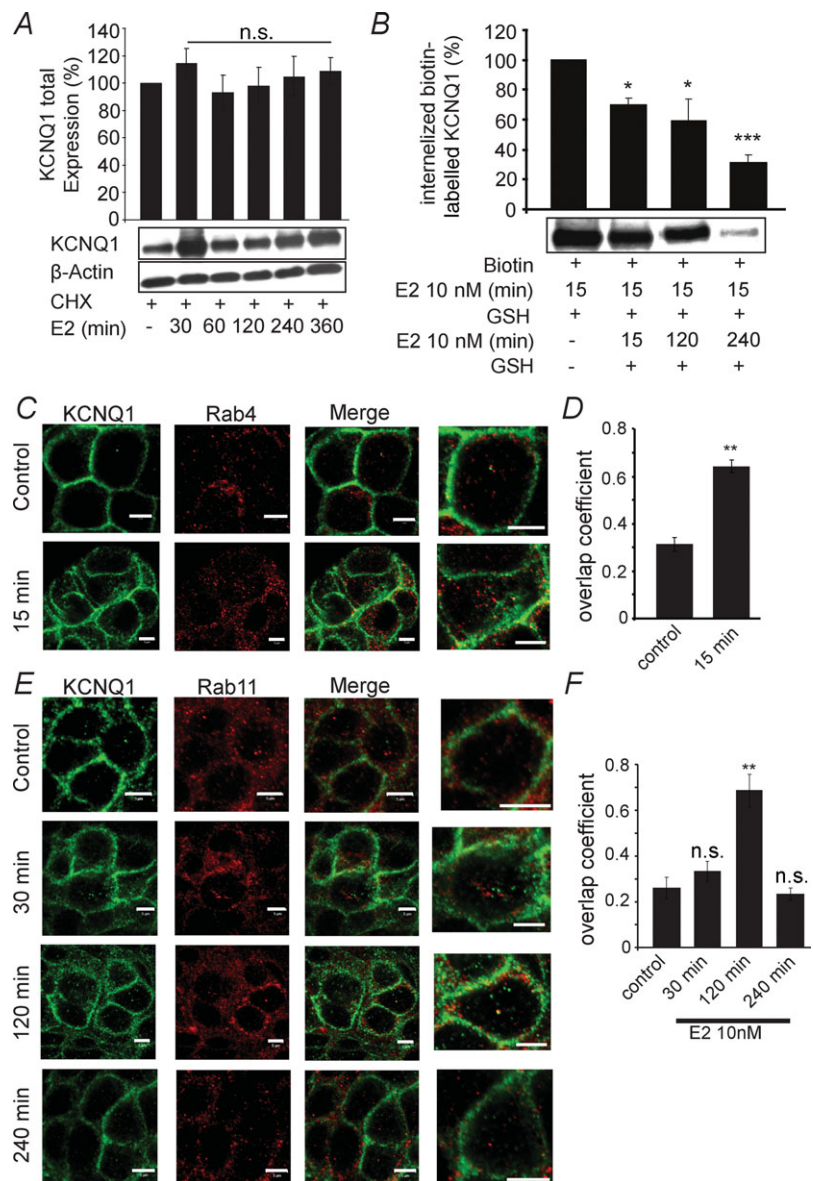


**Figure 5. Postendocytic fate of KCNQ1 following 17β-oestradiol exposure**

**A**, total protein expression of KCNQ1 in HT29cl.19A cells after indicated times of E<sub>2</sub> treatment. Cells were treated with cycloheximide (CHX; 100 μM) to prevent protein neosynthesis. The Western blot shown is representative of four independent experiments. **B**, biotin recycling assays were performed as follows. Cells were biotinylated at 4°C and then treated with E<sub>2</sub> for 15 min in the incubator to allow KCNQ1 to be internalized, after which the remaining surface biotin was removed by incubation in glutathione (GSH) buffer on ice. Cells were then incubated at 37°C in the presence of E<sub>2</sub> for the indicated times to allowed proteins to recycle. After incubation, surface biotin was removed using GSH buffer. Samples were then subjected to a Western blot to detect internalized KCNQ1 (\**P* < 0.05, \*\*\**P* < 0.001, *n* = 6). **C**, confocal images show KCNQ1 (green) and Rab4 (red) colocalization before and after 15 min E<sub>2</sub> treatment. Images are representative of four different experiments. Scale bars represent 5 μm. **D**, quantification of KCNQ1 and Rab4 colocalization using the overlap coefficient (\*\**P* < 0.01, *n* = 4). **E**, confocal images show KCNQ1 (green) and Rab11 (red) colocalization before and after 30, 120 and 240 min of E<sub>2</sub> treatment. Images are representative of four different experiments. Scale bars represent 5 μm. **F**, quantification of KCNQ1 and Rab11 colocalization using the pixel overlap coefficient.

HT29cl.19A cells with or without pretreatment with kinase inhibitors. Bisindolylmaleimide-1 (BIS-1; 5  $\mu$ M) has been used as a general PKC inhibitor and rottlerin (Rot; 5  $\mu$ M) as a PKC $\delta$  inhibitor. Finally, we used dorsomorphin (Comp-C; 20  $\mu$ M) as a specific AMPK inhibitor. Images revealed that E<sub>2</sub> failed to induce KCNQ1 endocytosis in HT29cl.19A cells when pretreated with BIS-1, rottlerin or compound-C (*n* = 4).

In order to confirm this result, we used the cell surface biotinylation assay (Fig. 6D). These experiments showed that KCNQ1 protein abundance at the surface membrane was reduced by 55% upon 15 min oestrogen treatment.

This effect was completely reversed when cells were pretreated with BIS-1, rottlerin or compound-C.

Finally, we tested whether E<sub>2</sub>-activated PKC and AMPK phosphorylation could be interdependent by using Western blotting assay of AMPK phosphorylation after 5 min of E<sub>2</sub> treatment in the presence or absence of PKC inhibitors. When cells were treated with E<sub>2</sub>, the AMPK phosphorylation increased by 250%. When HT29cl.19A cells were pretreated with BIS-1 or rottlerin, E<sub>2</sub> failed to activate AMPK phosphorylation (Fig. 6E). These results suggest that PKC $\delta$  activation is required for the E<sub>2</sub>-induced AMPK phosphorylation.

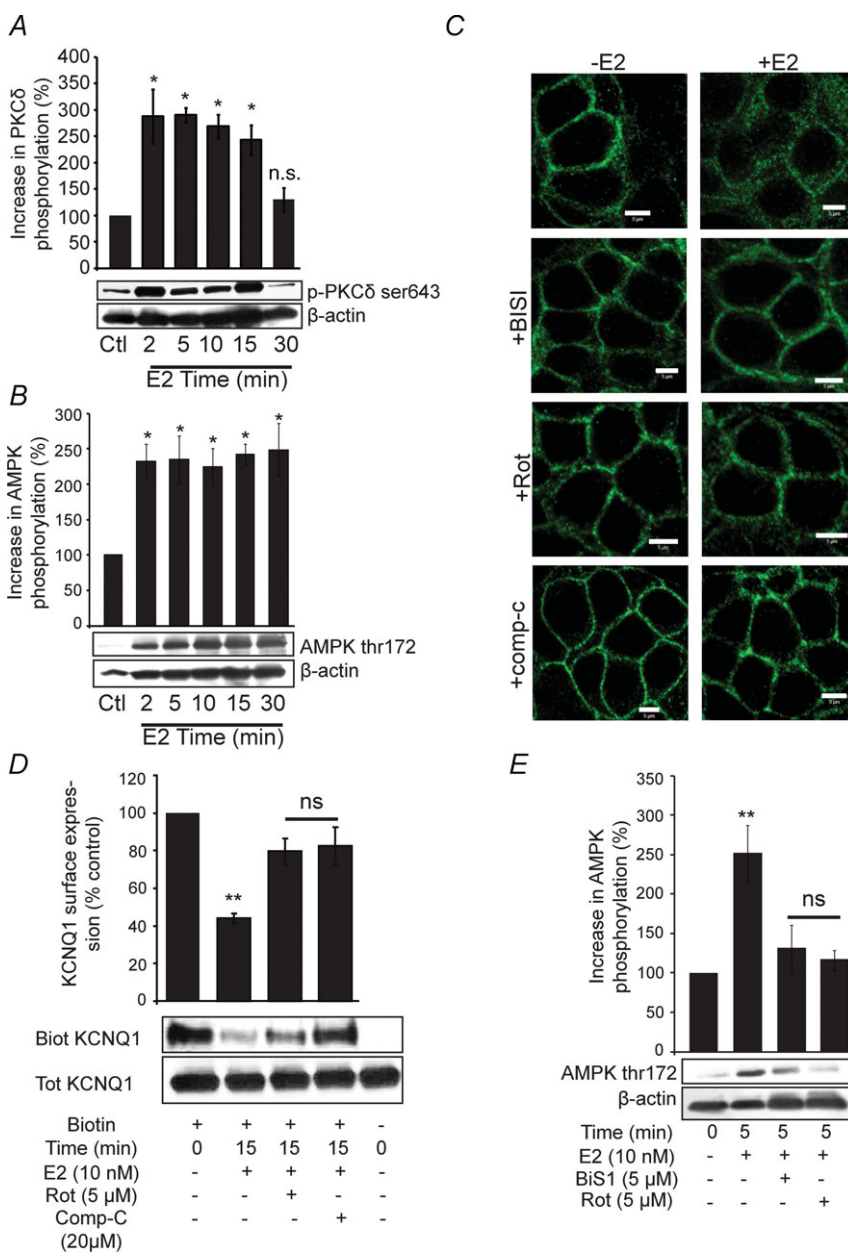


**Figure 6. 17 $\beta$ -oestradiol-induced internalization of KCNQ1 is dependent on activation of protein kinase C $\delta$  (PKC $\delta$ ) and AMP-dependent kinase (AMPK)**  
**A**, HT29cl.19A cells were treated with E<sub>2</sub> for the indicated times and then probed by Western blot assay using a specific antibody for phosphorylated (p)-PKC $\delta$  (*n* = 4, \**P* < 0.05). **B**, cells were treated with E<sub>2</sub> for the indicated times, and activated p-AMPK was assayed using a specific antibody by Western blotting (*n* = 5, \**P* < 0.05). **C**, confocal images from HT29cl.19A monolayers treated with E<sub>2</sub> without pretreatment or pretreated with kinase inhibitors, bisindolylmaleimide-1 (BIS-1; general PKC inhibitor; 5  $\mu$ M), rottlerin (Rot; specific PKC $\delta$  inhibitor; 5  $\mu$ M) or compound-C (Comp-C; specific AMPK inhibitor; 20  $\mu$ M). Images are representative of four independent experiments. Scale bars represent 5  $\mu$ m. **D**, Western blot analysis of KCNQ1-biotinylated proteins in HT29cl.19A cells treated with E<sub>2</sub> for 15 min and in the absence or presence of inhibitors (30 min pretreatment) BIS-1, rottlerin or compound-C (*n* = 5, \*\**P* < 0.01). **E**, Western blot analysis of AMPK phosphorylation in HT29cl.19A cells after 5 min E<sub>2</sub> treatment with or without 30 min pretreatment with PKC inhibitors (BIS-1 or Rottlerin; *n* = 4, \*\**P* < 0.01).

### Oestrogen stimulates a rapid increase in KCNQ1–Nedd4.2 association

The E3 ubiquitin ligase Nedd4.2 has been previously shown to be involved in regulation of the surface density of KCNQ1 in cardiomyocytes (Jespersen *et al.* 2007). AMPK is known to regulate Nedd4.2 (Bhalla *et al.* 2006) and subsequently modulate ion channel internalization (Almaça *et al.* 2009; Alzamora *et al.* 2010; Alesutan *et al.* 2011*b*). We hypothesized that the E<sub>2</sub> activation of AMPK leads to Nedd4.2 activation and subsequent association with KCNQ1. In order to test this hypothesis, we performed a co-immunoprecipitation of KCNQ1 and Nedd4.2 following 5 min E<sub>2</sub> treatment. These experiments showed a rapid and large increase (by  $346 \pm 59\%$ ,  $n = 3$ ,  $P < 0.001$ ) in the association of KCNQ1 with Nedd4.2 after E<sub>2</sub> treatment (Fig. 7). This result suggests that after E<sub>2</sub> stimulation, AMPK activates Nedd4.2, after which the ubiquitin ligase associates with KCNQ1 to induce its internalization.

### Oestrogen stimulates rapid KCNE3 recycling

KCNQ1 may be retrieved from the membrane on its own or together with its regulatory subunit, KCNE3. We determined the fate of KCNE3 during the rapid phase of KCNQ1 internalization, up to 30 min post-oestrogen. Immunofluorescence confocal imaging of KCNE3 antibody revealed that KCNE3 remains stable in the plasma membrane in the absence of E<sub>2</sub> and undergoes rapid removal from the membrane within 15 min exposure to E<sub>2</sub>. The rapidly retrieved KCNE3 goes to early endosomes, from where it is quickly returned to the plasma membrane within 30 min (Supporting information, Fig. S2).

### Discussion

The present study determined the molecular mechanisms for sustained E<sub>2</sub>-induced modulation of the activity of the K<sup>+</sup> channel KCNQ1 and analysed the role of 17β-oestradiol in KCNQ1 membrane trafficking in

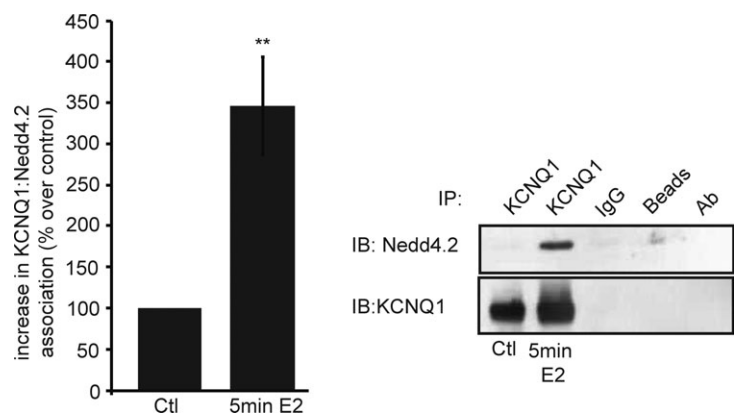
colonocytes. We obtain the following key findings. (i) Exposure to E<sub>2</sub> leads to a decrease in both Cl<sup>-</sup> secretion and KCNQ1 current. This inhibition seems to be maintained by a rapid and sustained retrieval of the channel from the plasma membrane. (ii) The E<sub>2</sub>-stimulated internalization of KCNQ1 occurs via a dynamin- and clathrin-dependent mechanism. (iii) KCNQ1 is recycled via Rab4 and Rab11 back to the membrane rather than being degraded. (iv) The signalling pathway activated by E<sub>2</sub> and leading to KCNQ1 internalization involves a signalling cascade where the activation of PKCδ induces the phosphorylation of AMPK. (v) 17β-oestradiol stimulated an increase in the association of KCNQ1 with the E3 ubiquitin ligase Nedd4.2. These findings provide evidence for a hormone-stimulated regulation of the surface density of KCNQ1 in colonic epithelium. Moreover, this study complements the understanding of the mechanisms for E<sub>2</sub>-induced inhibition of KCNQ1 previously described and provides new insights on hormonal regulation of ion channel retrieval from the plasma membrane.

### Oestrogen stimulates KCNQ1 inhibition and internalization

The role of the KCNQ1 channel in Cl<sup>-</sup> secretion has been disputed (Liao *et al.* 2005); however, a recent study (Preston *et al.* 2010) clearly demonstrated, using KCNE3 knockout mice, that the complex KCNQ1:KCNE3 plays a major role in cAMP-stimulated Cl<sup>-</sup> secretion in the intestine. 17β-oestradiol has previously been shown to exert an inhibitory effect on forskolin-stimulated Cl<sup>-</sup> secretion in female rat colonic crypts (Condliffe *et al.* 2001). In the present study, we demonstrated that E<sub>2</sub> reduces Cl<sup>-</sup> secretion evoked by forskolin in HT29cl.19A epithelial monolayers. We have previously shown that E<sub>2</sub> inhibits the forskolin-stimulated Cl<sup>-</sup> secretion in rat distal colon when added either before or during the forskolin response (Condliffe *et al.* 2001). The time course of E<sub>2</sub> inhibition of Cl<sup>-</sup> secretion (within 5 min) corresponds to the onset of KCNQ1 internalization.

#### Figure 7. 17β-oestradiol stimulates a rapid increase in the association of KCNQ1 with Nedd4.2

Protein samples from HT29cl.19A cells treated for 5 min with oestrogen (10 nM) or in vehicle control solution were subjected to immunoprecipitation using a specific KCNQ1 antibody. A Western blot was carried out to detect Nedd4.2. KCNQ1 was used as a loading control to normalize Nedd4.2 for quantification. Different controls were used to ensure the quality of the co-immunoprecipitation, as follows: KCNQ1 antibody was added to the beads without proteins (Ab); beads were incubated with proteins but without antibody (Beads); and rabbit IgG was added to the beads in place of KCNQ1 antibody, then incubated with proteins (IgG). Values are shown as normalized means + SEM; \*\* $P < 0.01$ ,  $n = 3$ . Abbreviations: IB, immunoblot; and IP, immunoprecipitation.



In rat colon, the antisecretory response to oestrogen has been attributed to an inhibition of KCNQ1 (O'Mahony *et al.* 2007). In the present study, we also showed that KCNQ1 current is reduced after a short  $E_2$  exposure of 15 min (Fig. 1). Interestingly, when cells are treated for 2 h with  $E_2$ , the KCNQ1  $K^+$  current remained reduced, at a value comparable to that after 15 min. The molecular mechanism for the inhibition of KCNQ1 by  $E_2$  has been investigated previously (Alzamora *et al.* 2011a).  $17\beta$ -oestradiol induced a dissociation between KCNQ1 and KCNE3, leading to the channel inhibition.

However, considering the sustained effect of  $E_2$  on KCNQ1 current inhibition, different hypotheses can be addressed. Firstly, the effect of  $E_2$  could prevent a reassociation between KCNQ1 and KCNE3. Secondly,  $E_2$  could lead to a subsequent internalization of KCNQ1, followed by channel degradation or sequestration in sub-cellular compartments. The present study investigated the latter hypothesis.  $17\beta$ -oestradiol has already been reported to stimulate the internalization of membrane proteins, such as the LPA1 receptor (González-Arenas *et al.* 2008). Recently, several ion channels have been shown

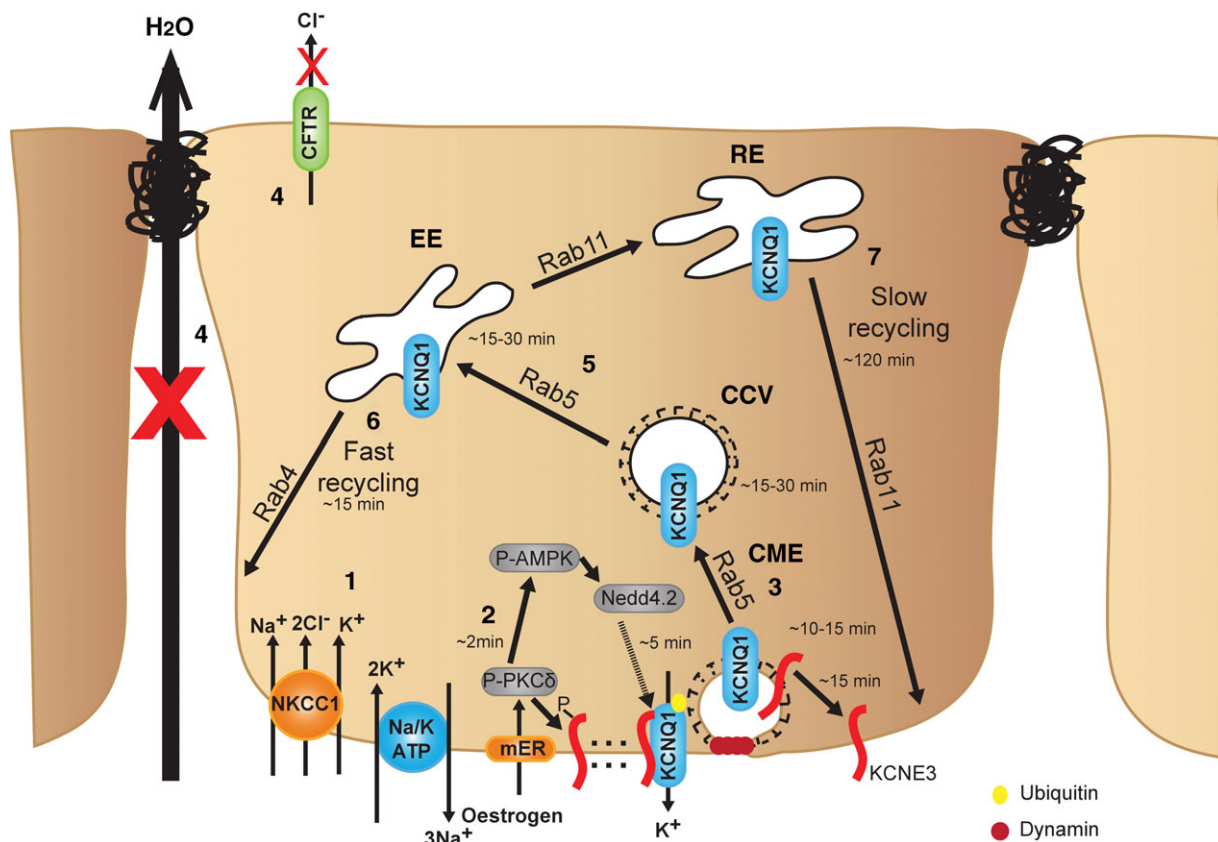


**Figure 8. Proposed mechanism for  $17\beta$ -oestradiol-induced internalization of KCNQ1 and consequences for  $Cl^-$  secretion in colonocytes**

(1) In colonocytes,  $Cl^-$  secretion is regulated by the concerted action of different apical and basolateral membrane ion channels and transporters, which promote vectorial apical fluid secretion. (2)  $E_2$ , acting via a membrane-associated  $ER\alpha$  receptor, rapidly activates a signalling pathway involving the phosphorylation of  $PKC\delta$  and AMPK. AMPK in turn activates Nedd4.2, which then binds and ubiquitinylates KCNQ1 to cause its internalization.  $17\beta$ -oestradiol, via  $PKC\delta$ , induces the dissociation between KCNQ1 and KCNE3 to reduce channel conductance. (3) The ubiquitinylated KCNQ1 is internalized through a clathrin-mediated mechanism. (4) The combined effect of KCNQ1:KCNE3 dissociation and retrieval of KCNQ1 from the plasma membrane reduces the electrical driving force for apical  $Cl^-$  secretion by the inhibition of basolateral  $K^+$  recycling. The inhibition of  $Cl^-$  secretion leads to a decrease in fluid secretion. (5) KCNQ1 internalization is mediated by Rab5; the channel is accumulated in early endosomes (EEs). (6) A subset of KCNQ1 channels is subjected to a fast recycling via Rab4. (7) Another pool of endocytosed KCNQ1 is sequestered into recycling endosomes (REs) and finally recycled back to the plasma membrane via Rab11. This complex recycling mechanism allows the cell to finely tune  $Cl^-$  secretion via modulation of the KCNQ1 surface abundance. CCV, Clathrin coated vesicles; CME, clathrin mediated endocytosis; CFTR, Cystic fibrosis transmembrane conductance regulator; NKCC1, Na-K-Cl Cotransporter 1; mER, membrane-associated oestrogen receptor; Nedd4.2, neural precursor cell-expressed developmentally down-regulated protein 4.2.

to undergo internalization after hormonal stimulation. For example, insulin enhances internalization of renal outer medullary potassium channel (Cheng & Huang, 2011), and angiotensin II induces internalization of  $K_{ATP}$  channels through PKC activation (Jiao *et al.* 2008). In the present study, we demonstrate that  $E_2$  enhances KCNQ1 endocytosis in both female rat colonic crypts and HT29cl.19A colonic cells after 15–30 min of treatment. We used two different approaches to study the effect of  $E_2$  exposure on endogenous KCNQ1 membrane trafficking, namely immunostaining and internalization biotin assays, in two different epithelia, HT29cl.19A monolayers and isolated rat colonic crypts. We observed a clear internalization of KCNQ1 that could provide an explanation for the prolonged  $E_2$  inhibitory effect on KCNQ1 current observed in Ussing chamber experiments.

Previous studies have shown that oestrogen uncouples KCNQ1 from KCNE3 (Alzamora *et al.* 2011a), but there are no reports of concurrent trafficking of both channel complexes. In the present study, we show a rapid and transient retrieval of KCNE3 induced by short-term exposure to oestrogen over 30 min. KCNE3 localizes to early endosomes within 15 min but is quickly returned to the plasma membrane (Supporting information, Fig. S2). Given that the distances between the uncoupled KCNQ1 and KCNE3 are on the molecular scale, we assume that both channel complexes are retrieved simultaneously, with KCNE3 being returned to the membrane from the early endosomal compartment and perhaps acting as an anchoring recognition site for the latent membrane reinsertion of KCNQ1 to form functional channels.

### Molecular mechanism of oestrogen-induced KCNQ1 internalization

Endocytosis occurs through three different mechanisms, namely clathrin-mediated endocytosis, caveolin-mediated endocytosis and clathrin- and caveolin-independent endocytosis (McMahon & Boucrot, 2011). The small GTPase dynamin, which is essential in the separation of the endocytic vesicle from the plasma membrane, takes part in both clathrin-mediated endocytosis and caveolin-mediated endocytosis. Several potassium channels have been described to use dynamin and clathrin-mediated endocytosis for internalization (Bruederle *et al.* 2011). Abbott's group showed in two studies that dynamin and clathrin-mediated endocytosis are involved in KCNQ1 endocytosis when coexpressed with KCNE1 in heterologous systems (Xu *et al.* 2009; Kanda *et al.* 2011). In the present study, we showed a similar dynamin- and clathrin-mediated endocytosis mechanism for endogenous KCNQ1 internalization in colonocytes. The small GTPase Rab5 has been described to mediate KCNQ1 endocytosis in transfected *Xenopus laevis* oocytes and COS-7 cells (Seebom

*et al.* 2007). In the present study, we demonstrated that KCNQ1 rapidly associates with Rab5 after  $E_2$  stimulation, leading to accumulation of KCNQ1 in early endosomes. Thus, clathrin-mediated endocytosis and Rab5 seem to constitute a conserved mechanism for KCNQ1 endocytosis in different tissues.

### KCNQ1 postendocytic trafficking is orchestrated by Rab4 and Rab11

Endocytosed proteins can recycle back to the membrane or proceed to degradation in the lysosome. Recycling is a complex mechanism, which can be regulated by different second messengers (van de Graaf *et al.* 2008) or kinases (Seebom *et al.* 2007) and involve different Rab proteins. There are two main routes for the endocytosed protein to be recycled back to the membrane. The fast recycling route is mediated by Rab4, and the protein is rapidly recycled from the sorting endosome to the plasma membrane. The slow recycling route can involve two different pathways. The first pathway is a direct pathway controlled by Rab11, where the protein travels from the sorting endosome to the recycling endosome and then to the plasma membrane. The second pathway is more complex and involves transit of the protein to the trans-Golgi network before recycling to the membrane and is controlled by Rab9 and Rab11 (Somsel Rodman & Wandinger-Ness, 2000). In the present study, we demonstrate that KCNQ1 was not significantly degraded but was mainly recycled to the plasma membrane. Different studies have reported a similar preference for recycling after ion channel endocytosis (Hardel *et al.* 2008; van de Graaf *et al.* 2008). In particular, KCNQ1 has been reported to be recycled rather than degraded following internalization (Seebom *et al.* 2007). Nevertheless, another study reported both the internalization and degradation of KCNQ1 during the initial phase of the Madin-Darby canine kidney cell polarization (Andersen *et al.* 2012).

Interestingly, in the present study, we observed a complex recycling pattern. Indeed, the biotinylation recycling assay revealed a biphasic recycling of KCNQ1 after  $E_2$ -induced endocytosis. A first pool of KCNQ1 seems to be rapidly recycled within 15 min. Another time point assay performed 120 min after internalization showed no significant difference with the 15 min time point. Thus, at 2 h after internalization, approximately 30% of the endocytosed KCNQ1 was recycled back to the membrane. This finding was correlated with a significant increase in KCNQ1 and Rab4 colocalization after 15 min. Another pool of KCNQ1 seems to be sequestered, because after 240 min 70% of endocytosed KCNQ1 was recycled back to the membrane. This pool of KCNQ1 had been sequestered inside the cells for 4 h. The colocalization between Rab11 and KCNQ1 was increased compared with the control 120 min after  $E_2$  treatment and was decreased again after

240 min. Taken together, our results strongly suggest that a pool of KCNQ1 is sequestered in sorting endosomes or in the trans-Golgi network, from where it goes to the recycling endosome prior to returning to the plasma membrane, while another pool of internalized KCNQ1 is rapidly recycled back to the membrane. Other studies have demonstrated that the recycling events are not passive but tightly regulated by kinases (Seeböhm *et al.* 2007). Interestingly, a recent study demonstrated that Rab11 can be phosphorylated and activated by PKC (Pavarotti *et al.* 2012). It is possible that E<sub>2</sub> somehow regulates the different Rab proteins to activate a diversity of recycling pathways.

### Signalling pathways involved in the oestrogen-induced KCNQ1 endocytosis

We summarize our current understanding of oestrogen effects on KCNQ1:KCNE3 channel trafficking in Fig. 8. Although KCNQ1 undergoes a constitutive endocytosis (Fig. 2D), the E<sub>2</sub>-induced endocytosis of KCNQ1 is a stimulated event involving the activation of signalling cascades. The inhibition of KCNQ1 by oestrogen previously reported (O'Mahony *et al.* 2007) showed an involvement of PKC $\delta$ . Protein kinase C has been reported in several studies to support ion channel endocytosis (Jiao *et al.* 2008; Konopacki *et al.* 2011). Recently, it was demonstrated that KCNQ1:KCNE1 endocytosis is dependent on PKC (Kanda *et al.* 2011). Nevertheless, that study did not specify which isoforms of PKC were involved in endocytosis.

In the present study, we show that E<sub>2</sub> rapidly activated PKC $\delta$  by increasing its phosphorylation within 2 min. When pretreated with an inhibitor of PKC or an inhibitor of PKC $\delta$ , E<sub>2</sub> failed to induce KCNQ1 endocytosis. Caution must be exercised when interpreting results with PKC inhibitors. Although rottlerin has been used as a PKC $\delta$  inhibitor in hundreds of studies, its specificity has been called into question in cell-based assays (Soltoff, 2007). In previous studies, we have demonstrated that E<sub>2</sub> specifically activates PKC $\delta$  and no other serine threonine kinase to effect the antisecretory response (Condliffe *et al.* 2001; O'Mahony *et al.* 2007; O'Mahony & Harvey, 2008; Alzamora *et al.* 2011b), and KCNQ1 specifically binds to and is phosphorylated by PKC $\delta$  following E<sub>2</sub> treatment (O'Mahony *et al.* 2007, 2009). Thus, a rottlerin inhibitory effect on secretion (and KCNQ1 endocytosis) may be interpreted as specifically involving PKC $\delta$ . This conclusion is further supported by the rottlerin inhibition of the E<sub>2</sub>-induced PKC $\delta$  phosphorylation (Supporting information, Fig. S3).

Several studies reported that the AMPK could have a role in KCNQ1 internalization in different systems (Alzamora *et al.* 2010; Andersen *et al.* 2012). We addressed the hypothesis that AMPK could play a role in the signalling events leading to KCNQ1 endocytosis after E<sub>2</sub> stimulation.

Interestingly, E<sub>2</sub> activated AMPK rapidly within 2 min, similar to its effect on PKC $\delta$ . We showed that an AMPK inhibitor also reversed the E<sub>2</sub>-induced endocytosis of KCNQ1, which strongly suggests that AMPK is a key regulator of KCNQ1 endocytosis. It has been reported that AMPK and PKC $\delta$  could take part in the same signalling pathway directly (Turrell *et al.* 2011) or indirectly through liver kinase B1 (LKB-1) (Andersen *et al.* 2012). In the present study, we show that PKC $\delta$  activation is required for a rapid phosphorylation of AMPK and, once this is complete, the PKC $\delta$  phosphorylation is reversed. In this manner, PKC $\delta$  may be the rate-limiting component. AMPK must be activated for a longer duration to mediate the whole recycling process. Thus, AMPK is downstream of PKC $\delta$  in the endocytotic signalling pathway.

Interestingly, recent studies have proposed that following AMPK activation, the E3 ubiquitin ligase Nedd4.2 is activated and associates with KCNQ1 to ubiquitinate the channel and induce its endocytosis (Alzamora *et al.* 2010; Andersen *et al.* 2012). We show that E<sub>2</sub> strongly increased the association between KCNQ1 and Nedd4.2. Based on recent literature and our study, we speculate that following E<sub>2</sub>-induced PKC $\delta$  and AMPK activation, Nedd4.2 ubiquitinates KCNQ1, which is subsequently endocytosed.

### Physiological significance of oestrogen-modulated KCNQ1 trafficking

The regulation of ion channel surface density is a powerful mechanism to tune ion transport tightly and to modulate the physiological processes under the control of ion channel activity rapidly. Guo *et al.* (2009) provided evidence that the cell surface density of HERG is regulated by a physiological factor, extracellular K<sup>+</sup>, leading to a modulation of the cardiac action potential. The balance between ion channel membrane stability and endocytosis and the recycling cycle can constitute a powerful mechanism for rapid adaptation to, and sensing of, the extracellular environment (Markham *et al.* 2009). The capacity of the endocytic machinery to sequester proteins in a cytosolic compartment for a given time and then trigger latent recycling is a potent mechanism for temporal and spatial control of channel activity (Felicangeli *et al.* 2010).

This study describes a novel rapid hormonal regulation of KCNQ1 surface density in colonocytes, which can control KCNQ1 activity to modulate Cl<sup>-</sup> secretion. 17 $\beta$ -oestradiol induced the retrieval of KCNQ1 and its sequestration into an endocytic compartment for several hours after endocytosis. In the colon, this will have the effect of reducing Cl<sup>-</sup> and fluid secretion into the intestinal lumen. We have previously shown that oestrogen prevents Cl<sup>-</sup> secretion induced by bacterial toxins (Alzamora *et al.* 2011b), and in the present study we demonstrate that



channel endocytosis may underlie the sustained response. Furthermore, the antisecretory effect of oestrogen in the intestine is part of a wider whole-body response, involving the lung, kidney and sweat glands, to increase whole-body fluid volume in high-oestrogen states (Saint-Criq *et al.* 2012).

Although the uncoupling of KCNQ1 from KCNE3 and membrane retrieval of KCNQ1 can account for the rapid collapse in the electrical driving force for Cl<sup>-</sup> secretion and the sustained antisecretory response, respectively, we have shown that other transport proteins in the chloride secretory pathway are affected by oestrogen and the whole-body oestrogen status (O'Mahony *et al.* 2009). The study by O'Mahony *et al.* (2009) revealed that the antisecretory response is regulated throughout the female reproductive cycle and is primed by genomic regulation of the kinase PKC $\delta$ . For example, the expressions at gene and protein levels of the cystic fibrosis transmembrane regulator, Na<sup>+</sup>-K<sup>+</sup>-2Cl<sup>-</sup> cotransporter (NKCC1) and Na<sup>+</sup>-K<sup>+</sup>-ATPase are all reduced during long-term exposure (days) to high circulating oestrogen. This additional reduction in chloride secretory capacity ensures a prolonged antisecretory response over several days during the implantation window, and is most probably a major contributory factor to the increased extracellular fluid volume observed in oestrus.

## References

- Alesutan I, Föllner M, Sopjani M, Dërmaku-Sopjani M, Zelenak C, Fröhlich H, Velic A, Fraser S, Kemp BE, Seeböhm G, Völkl H & Lang F (2011a). Inhibition of the heterotetrameric K<sup>+</sup> channel KCNQ1/KCNE1 by the AMP-activated protein kinase. *Mol Membr Biol* **28**, 79–89.
- Alesutan I, Munoz C, Sopjani M, Dërmaku-Sopjani M, Michael D, Fraser S, Kemp BE, Seeböhm G, Föllner M & Lang F (2011b). Inhibition of Kir2.1 (KCNJ2) by the AMP-activated protein kinase. *Biochem Biophys Res Commun* **408**, 505–510.
- Almaça J, Kongsuphol P, Hieke B, Ousingsawat J, Viollet B, Schreiber R, Amaral MD & Kunzelmann K (2009). AMPK controls epithelial Na<sup>+</sup> channels through Nedd4-2 and causes an epithelial phenotype when mutated. *Pflugers Arch* **458**, 713–721.
- Alzamora R, Gong F, Rondanino C, Lee JK, Smolak C, Pastor-Soler NM & Hallows KR (2010). AMP-activated protein kinase inhibits KCNQ1 channels through regulation of the ubiquitin ligase Nedd4-2 in renal epithelial cells. *Am J Physiol Renal Physiol* **299**, F1308–F1319.
- Alzamora R, O'Mahony F, Bustos V, Rapetti-Mauss R, Urbach V, Cid PL, Sepúlveda FV & Harvey BJ (2011a). Sexual dimorphism and oestrogen regulation of KCNE3 expression modulates the functional properties of KCNQ1 K<sup>+</sup> channels. *J Physiol* **589**, 5091–5107.
- Alzamora R, O'Mahony F & Harvey BJ (2011b). Estrogen inhibits chloride secretion caused by cholera and *Escherichia coli* enterotoxins in female rat distal colon. *Steroids* **76**, 867–876.
- Andersen MN, Krzystanek K, Jespersen T, Olesen SP & Rasmussen HB (2012). AMP-activated protein kinase downregulates Kv7.1 cell surface expression. *Traffic* **13**, 143–156.
- Andersen MN, Olesen SP & Rasmussen HB (2011). Kv7.1 surface expression is regulated by epithelial cell polarization. *Am J Physiol Cell Physiol* **300**, C814–C824.
- Augeron C & Laboisse CL (1984). Emergence of permanently differentiated cell clones in a human colonic cancer cell line in culture after treatment with sodium butyrate. *Cancer Res* **44**, 3961–3969.
- Barrett KE & Keely SJ (2000). Chloride secretion by the intestinal epithelium: molecular basis and regulatory aspects. *Annu Rev Physiol* **62**, 535–572.
- Bendahhou S, Marionneau C, Haurogne K, Larroque MM, Derand R, Szuts V, Escande D, Demolombe S & Barhanin J (2005). In vitro molecular interactions and distribution of KCNE family with KCNQ1 in the human heart. *Cardiovasc Res* **67**, 529–538.
- Bhalla V, Oyster NM, Fitch AC, Wijngaarden MA, Neumann D, Schlattner U, Pearce D & Hallows KR (2006). AMP-activated kinase inhibits the epithelial Na<sup>+</sup> channel through functional regulation of the ubiquitin ligase Nedd4-2. *J Biol Chem* **281**, 26159–26169.
- Bruederle CE, Gay J & Shyng SL (2011). A role of the sulfonylurea receptor 1 in endocytic trafficking of ATP-sensitive potassium channels. *Traffic* **12**, 1242–1256.
- Cheng CJ & Huang CL (2011). Activation of PI3-kinase stimulates endocytosis of ROMK via Akt1/SGK1-dependent phosphorylation of WNK1. *J Am Soc Nephrol* **22**, 460–471.
- Condliffe SB, Doolan CM & Harvey BJ (2001). 17 $\beta$ -Oestradiol acutely regulates Cl<sup>-</sup> secretion in rat distal colonic epithelium. *J Physiol* **530**, 47–54.
- Feliciangeli S, Tardy MP, Sandoz G, Chatelain FC, Warth R, Barhanin J, Bendahhou S & Lesage F (2010). Potassium channel silencing by constitutive endocytosis and intracellular sequestration. *J Biol Chem* **285**, 4798–4805.
- González-Arenas A, Avendaño-Vázquez SE, Cabrera-Wrooman A, Tapia-Carrillo D, Larrea F, García-Becerra R & García-Sáinz JA (2008). Regulation of LPA receptor function by estrogens. *Biochim Biophys Acta* **1783**, 253–262.
- Guo J, Massaelli H, Xu J, Jia Z, Wigle JT, Mesaelli N & Zhang S (2009). Extracellular K<sup>+</sup> concentration controls cell surface density of I<sub>Kr</sub> in rabbit hearts and of the HERG channel in human cell lines. *J Clin Invest* **119**, 2745–2757.
- Hardel N, Harmel N, Zolles G, Fakler B & Klöcker N (2008). Recycling endosomes supply cardiac pacemaker channels for regulated surface expression. *Cardiovasc Res* **79**, 52–60.
- Heitzmann D & Warth R (2007). No potassium, no acid: K<sup>+</sup> channels and gastric acid secretion. *Physiology (Bethesda)* **22**, 335–341.
- Jespersen T, Grunnet M & Olesen SP (2005). The KCNQ1 potassium channel: from gene to physiological function. *Physiology (Bethesda)* **20**, 408–416.
- Jespersen T, Membrez M, Nicolas CS, Pitard B, Staub O, Olesen SP, Baró I & Abriel H (2007). The KCNQ1 potassium channel is down-regulated by ubiquitylating enzymes of the Nedd4/Nedd4-like family. *Cardiovasc Res* **74**, 64–74.

- Jiao J, Garg V, Yang B, Elton TS & Hu K (2008). Protein kinase C- $\epsilon$  induces caveolin-dependent internalization of vascular adenosine 5'-triphosphate-sensitive K<sup>+</sup> channels. *Hypertension* **52**, 499–506.
- Kanda VA, Purtell K & Abbott GW (2011). Protein kinase C downregulates I<sub>Ks</sub> by stimulating KCNQ1-KCNE1 potassium channel endocytosis. *Heart Rhythm* **8**, 1641–1647.
- Kirk KL & Dawson DC (1983). Basolateral potassium channel in turtle colon. Evidence for single-file ion flow. *J Gen Physiol* **82**, 297–329.
- Konopacki FA, Jaafari N, Rocca DL, Wilkinson KA, Chamberlain S, Rubin P, Kantamneni S, Mellor JR & Henley JM (2011). Agonist-induced PKC phosphorylation regulates GluK2 SUMOylation and kainate receptor endocytosis. *Proc Natl Acad Sci U S A* **108**, 19772–19777.
- Levin ER (2009). Plasma membrane estrogen receptors. *Trends Endocrinol Metab* **20**, 477–482.
- Liao T, Wang L, Halm ST, Lu L, Fyffe RE & Halm DR (2005). K<sup>+</sup> channel KVLQT1 located in the basolateral membrane of distal colonic epithelium is not essential for activating Cl<sup>-</sup> secretion. *Am J Physiol Cell Physiol* **289**, C564–C575.
- McMahon HT & Boucrot E (2011). Molecular mechanism and physiological functions of clathrin-mediated endocytosis. *Nat Rev Mol Cell Biol* **12**, 517–533.
- Manderfield LJ, Daniels MA, Vanoye CG & George AL Jr (2009). KCNE4 domains required for inhibition of KCNQ1. *J Physiol* **587**, 303–314.
- Manders EMM, Verbeek FJ & Aten JA (1993). Measurement of co-localization of objects in dual-colour confocal images. *Journal of Microscopy* **169**, 375–382.
- Markham MR, McAnelly ML, Stoddard PK & Zakon HH (2009). Circadian and social cues regulate ion channel trafficking. *PLoS Biol* **7**, e1000203.
- Marx SO, Kurokawa J, Reiken S, Motoike H, D'Armiento J, Marks AR & Kass RS (2002). Requirement of a macromolecular signaling complex for  $\beta$  adrenergic receptor modulation of the KCNQ1-KCNE1 potassium channel. *Science* **295**, 496–499.
- Melman YF, Krummerman A & McDonald TV (2002). KCNE regulation of KvLQT1 channels: structure–function correlates. *Trends Cardiovasc Med* **12**, 182–187.
- O'Mahony F, Alzamora R, Betts V, LaPaix F, Carter D, Irnaten M & Harvey BJ (2007). Female gender-specific inhibition of KCNQ1 channels and chloride secretion by 17 $\beta$ -estradiol in rat distal colonic crypts. *J Biol Chem* **282**, 24563–24573.
- O'Mahony F, Alzamora R, Chung HL, Thomas W & Harvey BJ (2009). Genomic priming of the antisecretory response to estrogen in rat distal colon throughout the estrous cycle. *Mol Endocrinol* **23**, 1885–1899.
- O'Mahony F & Harvey BJ (2008). Sex and estrous cycle-dependent rapid protein kinase signaling actions of estrogen in distal colonic cells. *Steroids* **73**, 889–894.
- Pavarotti M, Capmany A, Vitale N, Colombo MI & Damiani MT (2012). Rab11 is phosphorylated by classical and novel protein kinase C isoenzymes upon sustained phorbol ester activation. *Biol Cell* **104**, 102–115.
- Preston P, Wartosch L, Günzel D, Fromm M, Kongsuphol P, Ousingsawat J, Kunzelmann K, Barhanin J, Warth R & Jentsch TJ (2010). Disruption of the K<sup>+</sup> channel  $\beta$ -subunit KCNE3 reveals an important role in intestinal and tracheal Cl<sup>-</sup> transport. *J Biol Chem* **285**, 7165–7175.
- Prossnitz ER & Barton M (2011). The G-protein-coupled estrogen receptor GPER in health and disease. *Nat Rev Endocrinol* **7**, 715–726.
- Saint-Criq V, Rapetti-Mauss R, Yusef YR & Harvey BJ (2012). Estrogen regulation of epithelial ion transport: Implications in health and disease. *Steroids* **77**, 918–923.
- Schroeder BC, Waldegger S, Fehr S, Bleich M, Warth R, Greger R & Jentsch TJ (2000). A constitutively open potassium channel formed by KCNQ1 and KCNE3. *Nature* **403**, 196–199.
- Seeböhm G, Strutz-Seeböhm N, Birkin R, Dell G, Bucci C, Spinosa MR, Baltaev R, Mack AF, Korniyuchuk G, Choudhury A, Marks D, Pagano RE, Attali B, Pfeufer A, Kass RS, Sanguinetti MC, Tavaré JM & Lang F (2007). Regulation of endocytic recycling of KCNQ1/KCNE1 potassium channels. *Circ Res* **100**, 686–692.
- Soltoff SP (2007). Rottlerin: an inappropriate and ineffective inhibitor of PKC $\delta$ . *Trends Pharmacol Sci* **28**, 453–458.
- Somsel Rodman J & Wandinger-Ness A (2000). Rab GTPases coordinate endocytosis. *J Cell Sci* **113**, 183–192.
- Splawski I, Tristani-Firouzi M, Lehmann MH, Sanguinetti MC & Keating MT (1997). Mutations in the hminK gene cause long QT syndrome and suppress I<sub>Ks</sub> function. *Nat Genet* **17**, 338–340.
- Turrell HE, Rodrigo GC, Norman RI, Dickens M & Standen NB (2011). Phenylephrine preconditioning involves modulation of cardiac sarcolemmal K<sub>ATP</sub> current by PKC delta, AMPK and p38 MAPK. *J Mol Cell Cardiol* **51**, 370–380.
- van de Graaf SF, Rescher U, Hoenderop JG, Verkaar S, Bindels RJ & Gerke V (2008). TRPV5 is internalized via clathrin-dependent endocytosis to enter a Ca<sup>2+</sup>-controlled recycling pathway. *J Biol Chem* **283**, 4077–4086.
- Xu X, Kanda VA, Choi E, Panaghie G, Roepke TK, Gaeta SA, Christini DJ, Lerner DJ & Abbott GW (2009). MinK-dependent internalization of the I<sub>Ks</sub> potassium channel. *Cardiovasc Res* **82**, 430–438.
- Zadeh AD, Xu H, Loewen ME, Noble GP, Steele DF & Fedida D (2008). Internalized Kv1.5 traffics via Rab-dependent pathways. *J Physiol* **586**, 4793–4813.

### Author contributions

The experiments were carried out in the laboratories of the Department of Molecular Medicine, Royal College of Surgeons in Ireland, Dublin, Republic of Ireland. The contribution of each author was as follows: conception and design of the experiments, V.U. and B.J.H.; collection, analysis and interpretation of data, R.R.-M. and B.J.H.; drafting the article, R.R.-M. and B.J.H.; revising the article critically for important intellectual content, B.J.H., V.U., F.O'M. and F.V.S. All authors approved the final version of the manuscript.

### Acknowledgements

This work was supported by grants to B.J.H. from the Higher Education Authority of Ireland (PRTL Cycle 4) and a cotutelle support to R.R.-M. from the National Biophotonics Imaging Platform Ireland, the CNRS France and the University of Montpellier 1. CECs receives funding from the Centers of Excellence Base Financing Program of Conicyt Chile.

**Translational perspective**

Sex hormones play a physiological role in modulating the activity of many different types of ion channels. We have pioneered studies in the sexual dimorphism and oestrogen-mediated regulation of KCNQ1:KCNE3 channels underlying the basolateral membrane  $K^+$  current driving fluid secretion in the colon. Oestrogen-induced inhibition of  $Cl^-$  secretion is both rapid (by uncoupling the KCNQ1:KCNE3 channel complex) and sustained (sex differences in the expression of channels and other poorly understood oestrogen- and oestrous cycle-regulated mechanisms). We have found a novel and sustained oestrogen-induced regulation of KCNQ1 channel trafficking. So far, there are no data reporting the mechanisms for spontaneous or regulated KCNQ1 internalization in any tissue. Here, we determined the molecular mechanisms for oestrogen-induced internalization of KCNQ1 in colonic epithelial cells.